HHS Public Access

Author manuscript

Sci Signal. Author manuscript; available in PMC 2024 January 17.

Published in final edited form as:

Sci Signal. 2023 January 17; 16(768): eadd6702. doi:10.1126/scisignal.add6702.

A hepatokine derived from the ER protein CREBH promotes triglyceride metabolism by stimulating lipoprotein lipase activity

Hyunbae Kim[1], **Zhenfeng Song**[1], **Ren Zhang**[1], **Brandon S. J. Davies**[2], **Kezhong Zhang**[1,3,*]

[1]Center for Molecular Medicine and Genetics, Wayne State University School of Medicine, Detroit, MI 48201, USA

[2]Department of Biochemistry, Fraternal Order of Eagles Diabetes Research Center, and Obesity Research and Education Initiative, University of Iowa, Iowa City, IA 52242, USA

[3]Department of Biochemistry, Microbiology and Immunology, Wayne State University School of Medicine, Detroit, MI 48201, USA.

Abstract

The endoplasmic reticulum (ER)–tethered, liver-enriched stress sensor CREBH is processed in response to increased energy demands or hepatic stress to release an amino-terminal fragment that functions as a transcription factor for hepatic genes encoding lipid and glucose metabolic factors. Here, we discovered that the carboxyl-terminal fragment of CREBH (CREBH-C) derived from membrane-bound, full-length CREBH was secreted as a hepatokine in response to fasting or hepatic stress. Phosphorylation of CREBH-C mediated by the kinase CaMKII was required for efficient secretion of CREBH-C through exocytosis. Lipoprotein lipase (LPL) mediates the lipolysis of circulating triglycerides for tissue uptake and is inhibited by a complex consisting of angiopoietin-like (ANGPTL) 3 and ANGPTL8. Secreted CREBH-C blocked the formation of ANGPTL3-ANGPTL8 complexes, leading to increased LPL activity in plasma and metabolic tissues in mice. CREBH-C administration promoted plasma triglyceride clearance and partitioning into peripheral tissues and mitigated hypertriglyceridemia and hepatic steatosis in mice fed a high-fat diet. Individuals with obesity had higher circulating amounts of CREBH-C than control individuals, and human *CREBH* loss-of-function variants were associated with dysregulated plasma triglycerides. These results identify a stress-induced, secreted protein

*Corresponding author. kzhang@med.wayne.edu.

Author contributions: K.Z. designed and conducted the experiments, analyzed the data, and wrote the manuscript. H.K., Z.S., and B.S.J.D. performed the experiments, acquired the data, and analyzed the data. R.Z. provided the key reagents and critical comments.

Competing interests: H.K. and K.Z. are inventors on a patent application (WSU 22–1687) held/submitted by Wayne State University that covers the discovery of a stress-inducible hepatokine to boost triglyceride clearance and counteract hypertriglyceridemia. The other authors declare that they have no competing interests.

Data and materials availability: All data needed to evaluate the conclusions in the paper are present in the paper or the Supplementary Materials.

Supplementary Materials
This PDF file includes:
Figs. S1 to S8
Table S1 and S2
Other Supplementary Material for this manuscript includes the following:
MDAR Reproducibility Checklist
View/request a protocol for this paper from *Bio-protocol*.

fragment derived from CREBH that functions as a hepatokine to stimulate LPL activity and triglyceride homeostasis.

INTRODUCTION

Hypertriglyceridemia, a condition in which plasma triglyceride (TG) levels are elevated, precedes or coexists with major metabolic and cardiovascular diseases (CADs), such as type 2 diabetes (T2D), atherosclerosis, and nonalcoholic steatohepatitis (NASH) (1, 2). Clearance of plasma TG is primarily mediated by lipoprotein lipase (LPL) (3). LPL in the parenchymal cells of lipolytic tissues is transported to the lumens of capillaries by its endothelial cell transporter, glycosylphosphatidylinositol anchored high density lipoprotein binding protein 1 (GPIHBP1) (4, 5). LPL anchored to vascular endothelial cells by GPIHBP1 (6) hydrolyzes plasma TG, a process termed lipolysis, for local uptake into tissues. LPL activity is primarily controlled at the posttranslational level (7) and is regulated by interacting proteins, including three angiopoietin-like (ANGPTL) protein family members: ANGPTL3, ANGPTL4, and ANGPTL8 (8–11). ANGPTL3 is secreted by the liver as a complex with ANGPTL8 and regulates postprandial LPL activity in muscle and adipose tissues in an endocrine fashion (12, 13). Whereas the production of ANGPTL3 is insensitive to feeding or fasting, the synthesis of ANGPTL8 is highly induced by feeding (14–16). ANGPTL4, which is primarily secreted from adipose and liver tissues, inhibits peripheral LPL activity associated with adipose tissues to limit lipid storage under fasting (10, 12, 17, 18). Although substantial progress has been made, many aspects of how LPL activity and TG lipolysis and partitioning are fine-tuned remain to be elucidated.

CREBH (cyclic adenosine 3′,5′-monophosphate–responsive element-binding protein, hepatic-specific) is a type II membrane protein that is tethered to the endoplasmic reticulum (ER) and is a stress-sensing transcriptional regulator of energy homeostasis associated with hyperlipidemia, NASH, and atherosclerosis (14, 19–23). In response to inflammatory challenges, nutrient starvation, or circadian cues, CREBH transits from the ER to the Golgi, where it is processed by regulated intramembrane proteolysis (RIP) to release an N-terminal fragment that functions as a CREB transcription factor (24, 25). Activated CREBH drives expression of the genes encoding major metabolic regulators or enzymes involved in TG lipolysis (14, 21), fatty acid (FA) oxidation (14, 26), gluconeogenesis (27, 28), glycogenolysis (27), and hepatic autophagy (29). In particular, upon nutrient starvation, CREBH interacts with the nuclear receptors peroxisome proliferator–activated receptor α (PPARα) and PPARG coactivator 1 alpha (PGC1α) to synergistically drive expression of fibroblast growth factor 21, coactivators of TG lipolysis, regulators or enzymes involved in FA oxidation, and autophagosome components in the liver (26, 29, 30). In humans, patients with hypertriglyceridemia or atherosclerosis display high-rate nonsense mutations or rare genetic variant accumulation in the *CREBH* gene (20, 21).

The liver contributes to the endocrine control of whole-body metabolism by producing liver-derived secreted factors or hepatokines (31, 32). Hepatokines can act in isolation or in conjunction with other factors to coordinate systemic metabolic processes. Their concentrations and effects are altered in response to metabolic stressors, and dysregulation

in hepatokine production can lead to pathogenesis of obesity, T2D, and NASH. In this study, we revealed a pathway by which the ER-tethered CREBH protein is processed by RIP in the liver to produce a hepatokine that regulates LPL activity through interactions with ANGPTLs in response to energy demand. The identification of the CREBH-derived hepatokine provides insights into the functions and mechanisms underlying the interactions between hepatokines, ANGPTLs, and LPL and has important implications in therapeutic interventions whose goal is to control hyperglyceridemia and associated metabolic disorders.

RESULTS

CREBH is processed to release a C-terminal fragment that can be secreted into the circulation

We previously found that CREBH is processed by RIP to release its N-terminal fragment that acts as a transcription factor in liver hepatocytes under stress conditions (14, 24). CREBH is an ER-tethered, type II membrane protein with a single-pass transmembrane domain connected to its C terminus localized in the lumen of ER or Golgi (Fig. 1, A and B). In response to inflammatory challenges or energy demands, CREBH transits to the Golgi compartment, where it is cleaved by site 1 (S1P) and site 2 (S2P) proteases to release both a 36-kD N-terminal fragment (CREBH-N) and a 11-kD C-terminal fragment (CREBH-C) (Fig. 1A) (24). CREBH-N interacts with multiple distinct transcriptional regulators or nuclear receptors in a stress-dependent manner and transits to the nucleus to function as a transcription factor (19, 26). However, the fate of CREBH-C remains unexplored. To delineate the action and potential function of CREBH-C, we developed two rabbit polyclonal antibodies against full-length and/or cleaved CREBH proteins. Immunoblotting analysis with liver protein lysates from fed or fasted mice detected three forms of endogenous CREBH proteins in the livers of wild-type (WT) mice but not in those of CREBH-knockout (KO) mice after a 14-hour fast (Fig. 1C). The molecular weights matched with CREBH full-length, N-terminal, and C-terminal proteins, respectively. Western blot analysis using the CREBH-C–specific antibody detected increased CREBH-C protein signals in the blood sera of fasted WT mice (Fig. 1C). In comparison, CREBH-C signals in the livers or sera of fed WT mice were much lower. Next, we administered recombinant adenovirus overexpressing full-length CREBH (CREBH-F) or CREBH-C by tail vein injection to CREBH-KO mice. Secreted CREBH-C protein was steadily detected in the blood sera of CREBH-KO mice receiving adenovirus overexpressing or CREBH-C (Fig. 1D). Note that when CREBH-F was overexpressed, CREBH-F could be processed into its N- and C-terminal fragments in the liver even in the absence of stress stimuli (Fig. 1D). Together, these data suggest that CREBH-C derived from the CREBH-F can be secreted from the liver in response to fasting or overexpression of CREBH.

Next, we examined the presence of secreted CREBH-C in the blood sera of CREBH-KO and WT control mice fed an atherogenic high-fat (AHF) diet, which induces hepatic oxidative stress and ER stress, NASH, and atherosclerosis in murine models (14, 33, 34). When fed the AHF diet for 6 months, WT mice, but not KO mice, displayed increased levels of endogenous CREBH-C in the blood sera compared with mice fed a normal chow (NC) diet (Fig. 1E). Furthermore, CREBH-C was detected in the blood sera of both obese patients and

healthy controls (Fig. 1F), but at higher levels in those of obese individuals, suggesting a possible association of CREBH-C with obesity. We established a sandwich enzyme-linked immunosorbent assay (ELISA) to quantitatively determine CREBH-C concentrations in blood sera. In C57BL/6 WT mice, average serum CREBH-C concentrations were 19 to 23 ng/ml in the fed state and reached 56.16 ng/ml in the fasted state (Fig. 1G). After 6 months on the AHF diet, the average concentration of mouse serum CREBH-C was 41.2 ng/ml (Fig. 1G). In the blood sera of human patients with obesity, the concentrations of serum CREBH-C averaged 46.4 ng/ml, whereas the average concentration of serum CREBH-C in healthy individuals was 27.4 ng/ml (Fig. 1H).

Cleaved CREBH C terminus is secreted by exocytosis

Exocytosis is the key step of the secretory pathway for transporting lipids and proteins across the plasma membrane and involves secretory vesicles leaving the Golgi apparatus (35, 36). To test whether CREBH-C is secreted through the Golgi-dependent exocytotic pathway, we treated human hepatoma-derived 7 (Huh7) cells expressing a flag-tagged CREBH-F with the fasting hormone glucagon. Immunofluorescent staining showed that CREBH-C was located in the Golgi apparatus and transited into cytosolic puncta in Huh7 cells after glucagon treatment (Fig. 2A). The puncta positive for CREBH-C overlapped with vesicle-associated membrane protein 2 (VAMP2)-positive exocytotic vesicles, and a portion of these vesicles were dissipated within 4 hours of glucagon stimulation (Fig. 2A). These results suggested that the C terminus of CREBH was processed at the Golgi apparatus and then moved to exocytotic vesicles for secretion in response to energy demands triggered by glucagon stimulation. To further validate that CREBH secretion occurred through the exocytotic pathway, we performed immunoprecipitation–Western blot analysis in glucagon-treated Huh7 cells expressing CREBH-F or CREBH-C. No or trace levels of interaction between CREBH-C and the exocytotic vesicle components VAMP2, synaptosome-associated protein 25 (SNAP25), or soluble *N*-ethylmaleimide–sensitive factor attachment protein receptor (SNARE) (37, 38) were detected in vehicle-treated CREBH-F–expressing Huh7 cells (Fig. 2B). In contrast, interactions between CREBH-C and VAMP2, SNAP25, or SNARE were detected in glucagon-treated CREBH-F–expressing Huh7 cells. The interaction between CREBH-C and VAMP2 or SNAP25, but not SNARE, was detected in CREBH-C–expressing Huh7 cells treated with vehicle (Fig. 2B). However, in response to glucagon treatment, CREBH-C protein was detected in association with VAMP2, SNAP25, and SNARE in CREBH-F– or CREBH-C–expressing Huh7 cells. Together, these results suggest that CREBH-C liberated from CREBH-F is processed at the Golgi apparatus and moves to exocytotic vesicles for secretion upon glucagon stimulation.

CaMKII-mediated phosphorylation regulates the secretion efficiency of CREBH-C

We further investigated the regulatory mechanism of CREBH-C secretion from hepatocytes. Fasting or obesity can induce Ca^{2+} release from the ER, which subsequently activates the cytoplasmic Ca^{2+}-sensitive kinase CaMKII (Ca^{2+}/calmodulin dependent-protein kinase II) (39, 40). CaMKII regulates exocytosis by phosphorylating secretory vesicle components or cargo proteins (41, 42). CaMKII can also phosphorylate and activate transcription factors or nuclear receptors involved in metabolism, inflammation, and other cellular processes (39, 40, 43, 44). In both human and mouse CREBH protein, we identified three CaMKII

consensus phosphorylation sites (R-X-X-S/T), including Ser^{360}, Ser^{395}, and Thr^{429} (fig. S1A). In particular, the putative CaMKII phosphorylation sites Ser^{395} and Thr^{429} are within the CREBH C-terminal fragment released from S1P-catalyzed cleavage (fig. S1, A and B). To test whether a potential CaMKII-mediated CREBH phosphorylation is involved in secretion of CREBH-C, we substituted Ser^{360}, Ser^{395}, and Thr^{429} in the human CREBH protein with alanine using site-directed mutagenesis to generate the CREBH point mutants S360A, S395A, and T429A. We examined the production of intracellular or secreted CREBH-C from Huh7 cells expressing Flag-tagged WT CREBH or the point mutants and treated with glucagon or ionomycin, an intracellular calcium ionophore that stimulates CaMKII activity (45, 46). Glucagon or ionomycin stimulation induced the secretion of CREBH-C derived from WT CREBH, S360A CREBH, or T429A CREBH into culture media (Fig. 2C, middle and bottom). However, secretion of CREBH-C derived from S395A CREBH was detected to a lesser extent compared with that of WT CREBH or the other point mutants. These results suggested that CaMKII-mediated phosphorylation of CREBH at Ser^{395} may regulate the efficacy of CREBH-C secretion upon stimulation with glucagon or ionomycin. Note that the mutations in the putative CaMKII phosphorylation sites did not affect the production of the cleaved CREBH-C in cell lysates (Fig. 2C, top). Furthermore, immunoprecipitation–Western blot analysis showed that the CREBH-C–CaMKII interaction was readily detected in CREBH-C–expressing cells treated with glucagon or phosphate-buffered saline (PBS) (Fig. 2D). However, the CREBH-C–CaMKII interaction was detected in CREBH-F–expressing cells treated with glucagon but not with PBS (Fig. 2D). These results suggest that CaMKII can physically interact with CREBH-C and that CREBH-F must be processed to produce CREBH-C in response to glucagon stimulation before it can interact with CaMKII.

Secreted CREBH-C is transported into multiple metabolic organs and promotes plasma- and tissue-resident LPL activities and plasma TG clearance

To test whether the liver-derived CREBH-C can be transported to metabolically active organs, we administered a recombinant adenovirus expressing CREBH-C (Ad-CREBH-C) to CREBH-KO mice by tail vein injection. CREBH-C protein was detected in the livers, whole blood, white adipose tissue (WAT), skeletal muscle, hearts, and kidneys of CREBH-KO mice receiving Ad-CREBH-C (Fig. 3A). Further, as detected by immunohistochemical (IHC) staining, increased CREBH-C amounts were detected in multiple metabolic organs/tissues, including skeletal muscle, hearts, WAT, pancreases, and kidneys, of CREBH-KO mice receiving Ad-CREBH-C (Fig. 3B). These results suggested that CREBH-C can be secreted into the circulation and be retained in metabolically active tissues. Because CREBH-KO mice have a defect in lipolysis (14, 21), which is mediated by the enzyme LPL, we examined whether secreted CREBH-C was associated with the LPL complex in the circulation or in metabolic organs/tissues. Immunoprecipitation–Western blot analysis showed that CREBH-C was associated with the LPL complex in the metabolic organs where CREBH-C was retained, with relatively higher levels of association with resident LPL in skeletal muscle, heart, and WAT (Fig. 3C).

To determine the functional involvement of CREBH-C in LPL activity, we measured intravascular LPL activity in fasted mice that were treated with heparin to release LPL

into the blood. LPL activity in the postheparin treatment plasma of CREBH-KO mice was significantly decreased compared with that of WT mice (Fig. 3D). Furthermore, plasma LPL activity in blood samples from CREBH-KO mice expressing CREBH-C was significantly higher than that of CREBH-KO mice expressing green fluorescent protein (GFP) control (Fig. 3E). In line with the levels of CREBH-C associated with the resident LPL in the major metabolic organs/tissues (Fig. 3, B and C), the lipase activity of LPL in skeletal muscle, hearts, WAT, pancreases, and kidneys of CREBH-KO mice expressing CREBH-C was significantly higher than in those of CREBH-KO mice expressing GFP (Fig. 3, F to J). Together, these results suggested that CREBH-C increases plasma- or tissue-resident LPL activities. Moreover, the levels of serum TG in CREBH-KO mice expressing CREBH-C were significantly reduced (Fig. 3K), providing further evidence for a role of CREBH-C in promoting LPL activity and subsequent TG lipolysis and clearance. In addition, CREBH-C expression in CREBH-KO mice significantly decreased the serum levels of FA but increased those of β-hydroxybutyrate (BOH), the ketone body derived from FA mobilization (fig. S2, A and B). However, expression of CREBH-C did not significantly affect the levels of total serum cholesterol in CREBH-KO mice (fig. S2C).

CREBH-C interacts with ANGPTL3 and ANGPTL8 in the livers and blood sera of mice and humans

Activity of LPL is primarily controlled at the posttranscriptional level by ANGPTL family members through inhibitory interactions (8–10). ANGPTL3, which is constitutively produced by the liver, is complexed with feeding-inducible ANGPTL8 to modulate LPL activity in muscle and adipose tissue in an endocrine fashion (15, 16). We sought to determine whether CREBH-C is involved in the regulation of LPL by interacting with ANGPTLs. Immunoprecipitation–Western blot analyses showed that endogenous CREBH-C interacted with both ANGPTL3 and ANGPTL8 in blood sera and livers of WT mice but not in those of CREBH-KO mice. These interactions occurred under both fed and fasted conditions, although the interaction between CREBH-C and ANGPTL8 was reduced in response to fasting (Fig. 4, A and B). Next, we examined these interactions in mice fed an AHF diet, which induces hepatic oxidative and ER stress responses that are associated with NASH and atherosclerosis states (14, 33, 34). Although the interaction between CREBH-C and ANGPTL3 was detected in the livers or blood sera of WT mice fed either NC or the AHF diet, the interaction between CREBH-C and ANGPTL8 was detected to a greater extent in the livers or blood sera of mice fed the AHF diet (Fig. 4, C and D). In mouse primary hepatocytes treated with vehicle or palmitate (PA), a metabolic stressor that induces CREBH protein cleavage (14), immunofluorescent staining showed that CREBH-C was colocalized with ANGPTL3 or ANGPTL8 within the primary hepatocytes after PA treatment (fig. S3, A and B). These results suggest that energy demand caused by fasting or hepatic stress induced by the AHF diet or PA can promote the interaction of CREBH-C with ANGPTL3/8. Furthermore, interactions between secreted CREBH-C and ANGPTL3 or ANGPTL8 were detected in the sera of both obese patients and healthy controls (Fig. 4E). However, the interaction between CREBH-C and ANGPTL3 was increased in the blood sera of obese individuals, which was consistent with the increased levels of CREBH-C detected in this group (Fig. 1, F and H).

CREBH-C increases LPL activity by attenuating the inhibitory effect of ANGPTL3/8 on LPL

ANGPTL8 is complexed with ANGPTL3 to enhance the ability of ANGPTL3 to bind to and inhibit LPL, and this complex formation is required for efficient secretion of ANGPTL3 (12, 13). To test whether CREBH-C can disrupt ANGPTL3/8 complex formation, we examined the formation of ANGPTL3/8 complexes and the interaction between CREBH-C and ANGPTL3/8 in Huh7 cells expressing these proteins by immunoprecipitation–Western blot analysis. Although intracellular CREBH-C strongly interacted with ANGPTL3 and ANGPTL8 (Fig. 5, A and B), expression of CREBH-C, but not that of GFP, reduced the interaction between ANGPTL3 and ANGPTL8 (Fig. 5C). These data suggested that CREBH-C suppresses the formation of the ANGPTL3/8 complex by interacting with ANGPTL3 or ANGPTL8. Although the abundance of ANGPTL3 and ANGPLT8 in CREBH-C–expressing 293T cells was comparable to those in control cells (Fig. 5D), the protein ratio of ANGPTL8 to ANGPTL3, a reflection of the amounts of the ANPTL3/8 complex (10, 12), in the culture media was significantly reduced (Fig. 5, E and F). These results suggested that CREBH-C suppressed the formation of the ANGPTL3/8 complex. Next, we measured lipase activities of LPL after incubation with the culture media from 293T cells coexpressing various combinations of CREBH-C, ANGPTL3, and ANGPLT8 (Fig. 5, G and H). LPL activity was effectively suppressed by incubation with the media from cells expressing both ANGPTL3 and ANGPTL8 (Fig. 5I). However, the activity of LPL incubated with the media from cells coexpressing ANGPTL3 and ANGPTL8 with CREBH-C was significantly increased (Fig. 5I). Normalizing the percentage of LPL activity inhibition against the positive control demonstrated that the degree of LPL inhibition by ANGPTL3 and ANGPLT8 was significantly attenuated by the expression of CREBH-C (Fig. 5J). Together, these results indicated that CREBH-C promotes LPL activity by suppressing the formation of the ANGPTL3/8 complex and thus the inhibitory effect of ANGPTL3/8 on LPL activity.

Because CREBH activation requires S1P- and S2P-mediated proteolysis (24), we investigated the role of S1P and S2P in the ability of CREBH-C to regulate LPL. Whereas the media from control 293T cells transduced with CREBH-F attenuated the inhibitory effect of ANGPTL3/8 on LPL activity, the media from cells expressing CREBH-F with S1P or S2P knockdown failed to prevent the inhibitory effect of ANGPTL3/8 on LPL activity (fig. S4, A and B), suggesting that both S1P and S2P are required to generate CREBH-C to alleviate LPL inhibition by ANGPTL3/8. We next reconstituted CREBH-C, CREBH-N, or CREBH-F into CREBH-KO mouse primary hepatocytes using an adenoviral-based expression system. The lipase activity of LPL was enhanced by media conditioned by CREBH-KO hepatocytes reconstituted with CREBH-F compared with media conditioned by WT hepatocytes reconstituted with GFP (Fig. 5, K and L). Similarly, the lipase activity of LPL was also enhanced by media conditioned by CREBH-KO hepatocytes reconstituted with CREBH-C compared with media conditioned by CREBH-KO hepatocytes reconstituted with GFP or CREBH-N. However, the increase in LPL activity was enhanced to a greater extent by CREBH-F reconstitution compared with CREBH-C reconstitution, although the difference was statistically insignificant (Fig. 5, K and L). In contrast, reconstitution of CREBH-N into CREBH-KO hepatocytes only had a marginal effect in promoting LPL activity compared with GFP reconstitution. These results suggest that CREBH-C, but not

CREBH-N, plays a major role in promoting LPL activity and that the maximal enhancement of LPL activity requires both CREBH-C and CREBH-N, which are derived from the same molecule, CREBH-F.

CREBH-C interacts with ANGPTL3 or ANGPTL8 through the SE1 protein domain

To understand the molecular basis underlying the interactions between CREBH-C and ANGPTL3/8, we sought to identify the protein domains involved in the interaction between CREBH-C and ANGPTL3 or ANGPLT8. Both ANGPTL3 and ANGPLT8 have a conserved region called specific epitope 1 (SE1; LAXGLLXLGXGL) in the N-terminal domain of the protein (Fig. 6, A and B, and fig. S5) (47). The SE1 domain is required for LPL binding and inhibition by ANGPTL3/8 (13, 47). In addition, ANGPTL proteins, with the exception of ANGPTL8, share a similar molecular structure with an N-terminal coiled-coil (CC) and a C-terminal fibrinogen-like domain connected by a linker region (48). We constructed plasmid vectors encoding Myc-tagged CREBH-C or different isoforms of mouse ANGPTL3 or ANGPTL8, which included a full-length ANGPTL3 (ANGPTL3), a truncated ANGPTL3 lacking SE1 domain (amino acids 32 to 57) (ANGPTL3-SE1), a truncated ANGPTL3 lacking both SE1 (amino acids 32 to 57) and CC (amino acids 56 to 152) domains (ANGPTL3-SE1-CC), a full-length ANGPTL8 (ANGPTL8), and a truncated ANGPTL8 lacking the SE1 (amino acids 29 to 49) domain (ANGPTL8-SE1) (Fig. 6, A and B). Immunoprecipitation–Western blot analysis of 293T cells expressing these constructs showed that CREBH-C failed to form a complex with ANGPTL3 if the SE1 domain was deleted (ANGPTL3-SE1), whereas the interaction between CREBH-C and ANGPTL3 was not affected by the deletion of the CC domain from ANGPTL3 (ANGPTL3-CC) (Fig. 6A). Similarly, removal of the SE1 domain from ANGPTL8 prevented the interaction between CREBH-C and ANGPTL8 (Fig. 6B). These results indicated that the SE1 domain is required for the interaction between CREBH-C and ANGPTL3 or ANGPTL8.

CREBH-C suppressed hypertriglyceridemia, alleviated hepatic steatosis, and improved lipid partitioning into peripheral tissues in mice

To validate the links between CREBH and metabolic disorders in humans, we performed generalized human gene set analysis based on the Common Metabolic Diseases Knowledge Portal (CMDKP) comprising 271 datasets and 330 traits (https://hugeamp.org/). CREBH was among the top list of common variant gene-level associations for TG dysregulation in the human population (https://hugeamp.org/phenotype.html?phenotype=TG). In 265,000 human patients, 27 CREBH gene variants were associated with dysregulated TG levels ($P = 1.72 \times 10^{-9}$). The top loss-of-function CREBH single variant (variant rs350879) is associated with increased TG levels in human patients ($P = 1.08 \times 10^{-11}$). Our multi-trait analysis of human genome-wide association study (GWAS) identified that CREBH common gene variants were significantly associated with the major metabolic phenotypes, including elevated TG and LDL cholesterol levels as well as body mass index (BMI), in over 240,000 human patients (table S1). CREBH gene variants were correlated with an increased incidence of CAD in T2D ($P = 0.04406$). Furthermore, two loss-of-function mutations have been identified in exon 10 of the human *CREBH* gene (22, 49): *c.G1208A:p.W403X*, a nonsense mutation that results in a stop codon within the region encoding CREBH-C and therefore generates a truncated protein, and *c.C1108A:p.R370S*, a missense mutation within

the region encoding CREBH-C (fig. S6, A to C). Patients with either of these mutations exhibited higher plasma TG and cholesterol levels than control individuals (22). These analyses suggest that human *CREBH* loss-of-function variants, especially those that affect CREBH-C production, are associated with dysregulated plasma TG and higher prevalence of CAD and T2D.

Consistent with the link between CREBH impairment and TG-associated metabolic disorders in humans, CREBH-KO mice exhibit hyperlipidemia, NASH, lipoatrophy (diminished adipose tissue mass), and reduced body weight, and these phenotypes are exacerbated by a high-fat diet (HFD) (14, 20, 21, 26, 29). To validate whether CREBH can function as an LPL-boosting hepatokine to mitigate TG-associated metabolic disorders, we injected CREBH-KO mice fed a HFD with CREBH-C or GFP-encoding adenoviruses (Fig. 7A). Expression of CREBH-C significantly alleviated the hyperlipidemia phenotype of CREBH-KO mice fed a HFD by reducing serum levels of TG and FA (Fig. 7, B and C). However, CREBH-C expression did not affect the levels of total serum cholesterol in CREBH-KO mice (Fig. 7D). These results support a role of CREBH-C in plasma TG and FA clearance by promoting LPL activity and TG lipolysis (Fig. 3, D to K).

Next, we examined whether CREBH-C intervention promoted TG partitioning into major metabolic organs and tissues, a lipid redistribution process that coexists with TG lipolysis. In mice fed a HFD, CREBH-C expression alleviated hepatic steatosis but increased fat content in skeletal muscle and adipose tissues of CREBH-KO mice, as shown by oil red O staining of neutral lipids (Fig. 7E). Hematoxylin and eosin (H&E) staining showed that CREBH-C expression improved the tissue morphology of liver, muscle, and adipose tissues in HFD-fed CREBH-KO mice, as characterized by tissue cell size and density and tissue structure and thickness (Fig. 7F). Further, enzymatic-based quantitative analyses indicated decreased hepatic TG and FA contents and increased FA and TG contents in extrahepatic lipolytic organs/tissues, including skeletal muscle, heart, kidney, and pancreas, as well as increased subcutaneous fat mass in the CREBH-KO mice expressing CREBH-C compared with CREBH-KO mice expressing GFP (Fig. 7, G to M, and fig. S7, A and B). Consistent with the improved TG partitioning and storage in the peripheral tissues, CREBH-KO mice expressing CREBH-C weighed significantly more than those expressing GFP (Fig. 7N). In addition, gene expression analysis showed increased expression levels of genes encoding proteins involved in TG lipolysis, including ApoC2, ApoA4, and ApoA5, and in FA oxidation, including PPARα, Cpt1α, Bdh1, and Fads2, in the livers of mice expressing CREBH-C compared with those in GFP-expressing mice (fig. S8), confirming that CREBH-C overexpression stimulates the transcriptional programs involved in TG lipolysis and FA metabolism. Together, these data indicate that CREBH-C can promote plasma TG clearance, mitigate hypertriglyceridemia and hepatic steatosis, and increase FA uptake into skeletal muscle and adipose tissues.

DISCUSSION

We previously demonstrated that a cleavage product of CREBH, CREBH-N, functions as a transcription factor to activate expression of the genes encoding enzymes or regulators involved in lipid and glucose metabolic pathways. CREBH deficiency leads to hepatic

steatosis, hyperlipidemia, and lipoatrophy associated with NASH, atherosclerosis, and T2D in both animal models and human patients (table S1) (14, 19–23). However, it has been unclear how CREBH as a transcription factor can exert such a powerful and full spectrum regulation of whole-body metabolism, as we previously described. Here, we provide insight into this conundrum through our finding that the cleaved C terminus of CREBH functions as a hepatokine, or secreted protein factor from the liver, to regulate LPL activity (Fig. 7O). We showed that CREBH was processed to release its C terminus fragment, CREBH-C, that was secreted after phosphorylation by CaMKII through a Golgi-dependent exocytotic pathway from hepatocytes in response to fasting or glucagon stimulation. Secreted CREBH-C interacted with ANGPTL3 and ANGPTL8 in the livers and blood sera of fasted mice to suppress the formation of the ANGPTL3/8 complex and thus promote LPL activity. CREBH-C expression prevented hypertriglyceridemia, alleviated hepatic steatosis, and improved TG partitioning and fat storage to peripheral metabolic tissues by enhancing intravascular LPL activity. CREBH-C intervention may mitigate hyperlipidemia and the associated metabolic disorders caused by overnutrition.

The CREB3 family of transcription factors, which includes CREB3, CREB3L1, CREB3L2, CREBH, and CREB3L4, are ER-localized proteins that belong to the basic leucine zipper (bZIP) family (50, 51). In response to stimulation by specific signals, they are transported from the ER to Golgi, where their luminal domains are cleaved by S1P. This cleavage enables a second cleavage catalyzed by S2P, which liberates their N-terminal transcription activation domain from membranes, allowing it to enter the nucleus, where it functions as a transcription factor (52). Among the CREB3 family members, CREB3L2 can be processed to produce a secreted C terminus that stimulates proliferation of neighboring cells or axon growth (53, 54). Production and function of secreted CREB3L2 is S2P dependent, and axonal S2P activity liberating the secreted C terminus of CREB3L2 is required for axon growth (53). In combination with our previous work (14, 19, 24, 26, 27, 29), we demonstrated that, in response to energy demands or hepatic stress, CREBH is processed by RIP to produce two functional fragments (Fig. 7O). In addition to the CREBH N terminus, which functions as a transcription factor, RIP of CREBH generates the CREBH C terminus, which functions as a hepatokine to promote LPL activity and TG partitioning into peripheral tissues through posttranslational regulation. The functions of both N and C termini enable CREBH to robustly regulate systemic lipid homeostasis, which may be crucial to shaping metabolic flexibility upon stress challenges.

This work sought to address the function of CREBH-C. On the basis of our studies, the inhibitory effects of CREBH-C on the ANGPTL3/8 complex are likely achieved through two layers of interactions. The first is the interaction of intracellular CREBH-C with ANGPTL3 or ANGPTL8 in the liver to attenuate the formation and secretion of ANGPTL3/8 complex. The second is the interaction of secreted CREBH-C with ANGPTL3, ANGPTL8, or the ANGPTL3/8 complex in the circulation, thus preventing the inhibitory interaction between ANGPTL3/8 and LPL. After feeding, the combined action of ANGPTL3/8 reduces the clearance of plasma TG into brown adipose tissue, heart, and muscle, thereby rerouting plasma TG to WAT to replenish TG stores (8, 15). During fasting, the levels of ANGPTL3 and circulating ANGPTL8 remain high (10), but the remaining ANGPTL3/8 in the circulation must be suppressed so that plasma LPL activity is

enhanced to promote TG lipolysis and partitioning to meet the energy demands of oxidative tissues, such as skeletal muscle and heart. However, how the ANGPTL3 or ANGPTL3/8 activity is suppressed so that TG lipolysis and partitioning can be redirected upon fasting remains enigmatic. As suggested by our data, fasting induced the generation of CREBH-C to increase plasma LPL activity through inhibitory interactions with the remaining ANGPTL3 and ANGPTL8, thereby decreasing plasma TG levels. Regardless of whether mice were fasted or fed, CREBH-C overexpression mitigated hypertriglyceridemia and improved lipid partitioning into fat and muscle tissues (Figs. 3, D to K, and 7, B to N).

We confirmed the interaction between CREBH and ANGPTL3 or ANGPTL8 with human patient samples. Obese individuals exhibited increased levels of secreted CREBH-C associated with ANGPTL3 or ANGPTL8 in blood sera (Figs. 1F and 4E). Excessive production of secreted CREBH-C may be stimulated by obesity, because CaMKII, which is active in the fasted state or obesity (39, 40), promoted CREBH-C secretion (Fig. 2, C and D). It is possible that the increase in CREBH-C in obesity was compensatory to stimulate LPL-mediated TG lipolysis and partitioning into peripheral tissues when other factors have decreased lipolysis. Alternatively, metabolic disorders may impair CREBH-C function or stimulate CREBH-C overproduction, resulting in a “CREBH-C resistance” condition associated with metabolic syndromes such as hyperlipidemia/obesity, T2D, and atherosclerosis. The questions regarding the increase in CREBH-C with obesity warrant future investigations. In addition, our data have important implications in interventions to control LPL activity and TG homeostasis in peripheral tissues. Because LPL activity is primarily regulated by ANGPTLs, it is desirable to develop therapeutic interventions to counteract hypertriglyceridemia and the associated metabolic disorders by modulating ANGPTL activity. The ANGPTL3 monoclonal antibody evinacumab has been approved by the U.S. Food and Drug Administration to treat patients with homozygous familial hypercholesterolemia (11, 55). As shown by this work, CREBH-C acts as an endogenous inhibitor of ANGPTL3/8 or an enhancer of intravascular LPL activity. Stimulation of CREBH-C activity may represent an effective way to control hypertriglyceridemia by boosting TG lipolysis and uptake into peripheral tissues. These implications indicate that further investigation of the role of CREBH-C as a stress-induced hepatokine in metabolic diseases is warranted.

MATERIALS AND METHODS

Materials

Chemicals were purchased from Sigma-Aldrich unless indicated otherwise. Commercially available antibodies were used to detect ANGPTL3 (ABclonal), LPL (Proteintech), CaMKII (Santa Cruz Biotechnology), VAMP2 (Proteintech), GM130 (BD Transduction Laboratories), SNARE (Santa Cruz Biotechnology), SNAP25 (Abcam), S1P (ABclonal), S2P (Santa Cruz Biotechnology), and glyceraldehyde-3-phosphate dehydrogenase (GAPDH) (Sigma-Aldrich), respectively, in mouse livers by Western blot or by immunoprecipitation–Western blot analyses. Kits for measuring TGs and FAs were from BioAssay Systems. The kit for measuring LPL activity was from Cell Biolabs Inc. Rabbit polyclonal anti-CREBH antibody was raised by immunizing rabbits with a mouse CREBH

protein fragment spanning N-terminal amino acids 75 to 250 of mouse CREBH protein as previously described (26). Rabbit polyclonal antibodies directed against human or mouse CREBH-C protein were raised by immunizing rabbits with a mix (1:1) of a conserved human CREBH-C terminal peptide fragment (amino acids 364 to 382) and a mouse CREBH-C terminal peptide fragment (amino acids 360 to 379). The crude blood serum antibody was purified through affinity purification. A rabbit polyclonal mouse or human ANGPTL8 antibody was developed as previously described (56). The small interfering RNA (siRNA) against human S1P or S2P and scramble siRNA controls were from Thermo Fisher Scientific.

Human blood serum samples and Western blot analyses

To compare serum CREBH-C levels between human patients with or without obesity, blood serum samples collected from eight male healthy controls with BMI values of less than 25 and from eight male age-matched obese individuals with BMI values of more than 35 were used in the study. The deidentified human serum samples were purchased from Valley Biomedical Inc. (Winchester, VA) under Institutional Review Board exempt for biomedical research. For the Western blot analysis to detect serum CREBH-C, eight serum samples were pooled into two samples per group, and 2 μl of serum per sample were denatured for the analysis. For immunoprecipitation–Western blot analysis to detect interactions between CREBH-C and ANGPTL3/8, 3 μl of serum per sample were used for incubation with the primary CREBH-C antibody.

Mouse experiments

CREBH-KO mice of C57BL/6 strain background in which exons 4 to 7 of the *CrebH* gene were deleted were previously described (57). CREBH-KO and WT control mice of about 3 months of age on a C57BL/6 background were used for the experiments. For the metabolic diet study, mice were fed with a HFD (45% kcal fat) purchased from Research Diets Inc. (catalog no. D12451) for 4 weeks. For adenovirus injection experiments, recombinant adenovirus expressing the CREBH-C or GFP was injected into CREBH-KO mice through the tail vein. About 1×10^{10} plaque-forming units of adenovirus in 0.25 ml of PBS were intravenously injected into a mouse with a body weight of about 20 g. In addition, to examine the presence of CREBH-C in mice under metabolic stress, we fed C57BL/6 mice with an AHF diet (Paigen diet; 16% fat, 41% carbohydrate, 1.25% cholesterol, and 0.5% sodium cholate by weight) purchased from Harlan Laboratories Inc. (catalog no. TD.88051) for 6 months. All the animal experiments were approved by the Wayne State University Institutional Animal Care and Use Committee and carried out under the institutional guidelines for ethical animal use.

Nucleic acids and recombinant adenovirus vectors

The plasmid vectors expressing Flag-tagged CREBH-C, ANGPTL3, ANGPTL8, and their truncated forms under the control of the cytomegalovirus promoter were constructed and verified by sequencing of the insert regions. The sequences of the PCR primers used to generate truncated forms of mouse ANGPTL3 or ANGPTL8 are the following: 5′-AAAGATTTTGTCCATAAGACTAAGGGACAA-3′ and 5′- ATGGACAAAATCTTTTGAAGGTGCAGAATC-3′ were used to

generate ANGPTL3-SE1, 5′- GCTGGGGCTCAGGAGCACCCAGAAGTAACA-3′ and 5′- CTCCTGAGCCCCAGCATGACCCAGCTGCAG-3′ were used to generate ANGPTL3-CC, 5′-AAAGATTTTGTCCATAAGACTAAGGGACAA-3′ and 5′- CTCCTGAGCCCCAGCTGAAGGTGCAGAATC-3′ were used to generate ANGPTL3-SE1-CC, and 5′-AATGGCGTGTACAGAGCCACAGAGGCTCGC-3′ and 5′-TCTGTACACGCCATTCTCTGGACCACCCAGAG-3′ were used to generate ANGPTL8-SE1. Plasmids and recombinant adenovirus vectors expressing human CREBH-C, ANGPTL3, ANGPTL8, or GFP were constructed and verified by sequencing. High-titer ultrapure adenovirus particles for the animal experiments were prepared by VectorBuilder Inc. (Chicago, USA).

Cell culture and immunofluorescence analysis

Primary hepatocytes were isolated from WT or CREBH-KO mice on the C57BL/6 background as previously described (14). Primary hepatocytes were stimulated with 25 nM glucagon for the indicated amounts of time. For immunofluorescence analysis, cells grown on a glass coverslip were treated with 25 nM glucagon or vehicle for the indicated times, washed with PBS, and fixed with 4% formaldehyde. The fixed cells were incubated with the primary antibody overnight at 4°C and with Alexa Fluor 488– or Alexa Fluor 594–conjugated secondary antibody. Cells were then mounted with ProLong Gold Antifade reagent containing 4′,6-diamidino-2-phenylindole. The images were obtained with a Zeiss fluorescent microscope (Carl Zeiss, Germany).

Western blot and coimmunoprecipitation analyses

Equal amounts of denatured mouse liver protein lysates were run on SDS–polyacrylamide gels and transferred to polyvinylidene difluoride membranes. The blots were incubated with the primary antibody (1:1000 dilution) overnight at 4°C and with secondary antibody conjugated to horseradish peroxidase (1:10,000) for 1 hour at room temperature. For coimmunoprecipitation, 300 μg of protein extracts were incubated with 20 μl of protein A–agarose beads and 3 μg of a primary antibody in a total volume of 500 μl at 4°C overnight with rotation. After centrifugation, the supernatant containing nonbound protein was removed, and 1× sample buffer was added to the pellet. The eluted proteins were separated by SDS–polyacrylamide gel electrophoresis for Western blot analysis.

ELISA for CREBH-C

A sandwich ELISA was developed to measure concentrations of CREBH-C in the blood sera of mice or human patients. The rabbit polyclonal CREBH-C antibody developed as described above was used as the capture antibody (1:1000 dilution). Purified recombinant human CREBH-C protein was used to generate a standard curve. The sandwich immunoassay was performed using a DuoSet ELISA Development System (R&D Systems Inc.) according to the manufacturer’s instruction.

Measurement of LPL activity in peripheral tissues and plasma after heparin treatment

To measure resident LPL activities in peripheral tissues (skeletal muscle, heart, fat, kidney, and pancreas), about 50 mg of frozen tissue were homogenized with ice-cold PBS and

resuspended in LPL assay buffer as previously described (58). The tissue lysates were centrifuged at 15,000*g* for 15 min at 4°C to pellet cellular debris. Lipase activity assays were performed on the supernatants using an LPL enzymatic fluorometric assay kit (Cell Biolabs Inc.). To measure mouse plasma LPL activity, we treated CREBH-KO mice expressing CREBH-C or GFP were treated with heparin (1 U/g body weight) for 15 min to release LPL into the blood. Blood plasma samples from these mice were subjected to quantitative analysis of lipase activities of postheparin plasma LPL using a commercially available LPL enzymatic fluorometric assay kit.

Measurement of effect of CREBH-C or ANGPTL3/8 on LPL activity

293T cells (American Type Culture Collection, catalog no. CRL-3216) were cotransfected with the plasmid vector expressing both ANGPTL3 and ANGPTL8, the plasmid expressing CREBH-C, and/or the plasmid empty expression vector. Culture media were harvested at 48 hours after the transfection. The fresh culture media were incubated for 30 min at 37°C with human LPL, which was purified from the medium of an LPL-producing Chinese hamster ovary stable cell line as previously described (12). Samples were assayed for LPL lipase activity using a commercially available enzymatic fluorometric LPL assay kit (Cell Biolabs Inc.). LPL activity in the presence of medium from vector-transfected cells was used as the positive control for LPL activity to determine the degree of LPL inhibition by ANGPTL3 and ANGPTL8 in the presence or absence of CREBH-C and was presented as percentage of LPL activity.

TG and FA measurement in blood and tissue samples

To determine hepatic TG levels, about 20 mg of liver tissue were homogenized in PBS and centrifuged. The supernatant was mixed with 10% Triton X-100 in PBS for measurement of TG levels using a commercially available kit (BioAssay Systems). Mouse hepatic TG levels were determined by normalization to the mass of the liver tissue used for measurement of TG levels. Serum TG, FA, ketone body (BOH), and cholesterols [high-density lipoprotein (HDL) and low-density lipoprotein (LDL)/very-low-density lipoprotein (VLDL)] were measured using commercially available kits (BioAssay Systems). To measure tissue FA, 20 mg of tissue were homogenized in 200 μl of homogenization buffer (5% isopropanol and 5% Triton X-100 in water) and filtered through a 0.45-μm syringe filter. The levels of FAwere determined using a commercially available FA quantitative assay kit (BioAssay Systems).

Oil Red O staining

Frozen liver tissue sections were stained with Oil Red O for lipid contents according to standard protocol. Briefly, the frozen sections (12 μm) from optimal cutting temperature compound (OCT)–embedded livers were air-dried and fixed in 10% buffered formalin. The fixed slides were rinsed in 60% isopropanol and stained in Oil Red O solution. The slides were washed with 60% isopropanol and water and mounted in aqueous mounting media before being analyzed by microscopy.

Quantitative real-time PCR

Total RNA from mouse livers were extracted using the TRIzol reagent (Thermo Fisher Scientific), and cDNA was synthesized from 500 ng of total RNA with the High-Capacity cDNA Reverse Transcription Kit (Applied Biosystems). The abundance of mRNA was measured by quantitative real-time PCR analysis using the SYBR Green PCR Master Mix (Applied Biosystems). PCR was carried out using Applied Biosystems 7500 Real-Time PCR Systems. The sequences of the primer sets are listed in table S2.

Generalized gene set analysis of GWAS data

To identify the links between CREBH and major metabolic phenotypes, we performed generalized human gene set analysis based on the CMDKP comprising 271 datasets and 330 traits (https://hugeamp.org/). Specifically, the Metabolic Disorders Knowledge Portal was used to extract the results of mega-data analyses across multiple human patient datasets. The Metabolic Disorders Knowledge Portal outputs the common variant gene-phenotype associations by aggregating different GWAS for T2D datasets, each of which has *P* values and betas for single-nucleotide polymorphisms (SNPs). Meta-analysis was then performed to produce a single *P* value and beta for each SNP. Multi-marker Analysis of GenoMic Annotation (MAGMA), a tool for gene analysis and generalized gene set analysis of GWAS data (59), was run to convert the SNP-level statistics into gene-level statistics. The gene-phenotype results are generated by MAGMA method. The *P* values are summaries of the association strength of all SNPs within the specific gene. The numbers of variants correspond to the numbers of SNPs MAGMA examines, and the numbers of sample sizes correspond to the sample sizes output by MAGMA.

Statistics

Experimental results are shown as means ± SEM. In vitro experiments were repeated with biological triplicates at least three times independently. Mean values for biochemical data from the experimental groups were compared by unpaired two-tailed Student's *t* tests unless otherwise indicated. The differences were considered statistically significant if $P < 0.05$. Statistical analyses were conducted using Microsoft Excel or GraphPad Prism 9 software.

Supplementary Material

Refer to Web version on PubMed Central for supplementary material.

Acknowledgments:

We acknowledge R. Pique-Regi (Wayne State University) for guidance and verification of statistical tests used in this work.

Funding:

Portions of this work were supported by NIH grants DK090313 and DK126908 (to K.Z.), DK132065 (to R.Z. and K.Z.), HL130146 (to B.S.J.D.), and HL134787 (to R.Z.) and a Pilot and Feasibility Grant (to H.K.) from the Michigan Diabetes Research Center (NIH grant P30-DK020572).

REFERENCES AND NOTES

1. Subramanian S, Chait A, Hypertriglyceridemia secondary to obesity and diabetes. Biochim. Biophys. Acta 1821, 819–825 (2012). [PubMed: 22005032]
2. Do R, Willer CJ, Schmidt EM, Sengupta S, Gao C, Peloso GM, Gustafsson S, Kanoni S, Ganna A, Chen J, Buchkovich ML, Mora S, Beckmann JS, Bragg-Gresham JL, Chang H-Y, Demirkan A, Den Hertog HM, Donnelly LA, Ehret GB, Esko T, Feitosa MF, Ferreira T, Fischer K, Fontanillas P, Fraser RM, Freitag DF, Gurdasani D, Heikkilä K, Hyppönen E, Isaacs A, Jackson AU, Johansson Å, Johnson T, Kaakinen M, Kettunen J, Kleber ME, Li X, Luan J, Lyytikäinen L-P, Magnusson PKE, Mangino M, Mihailov E, Montasser ME, Müller-Nurasyid M, Nolte IM, O'Connell JR, Palmer CD, Perola M, Petersen A-K, Sanna S, Saxena R, Service SK, Shah S, Shungin D, Sidore C, Song C, Strawbridge RJ, Surakka I, Tanaka T, Teslovich TM, Thorleifsson G, Van den Herik EG, Voight BF, Volcik KA, Waite LL, Wong A, Wu Y, Zhang W, Absher D, Asiki G, Barroso I, Been LF, Bolton JL, Bonnycastle LL, Brambilla P, Burnett MS, Cesana G, Dimitriou M, Doney ASF, Döring A, Elliott P, Epstein SE, Eyjolfsson GI, Gigante B, Goodarzi MO, Grallert H, Gravito ML, Groves CJ, Hallmans G, Hartikainen A-L, Hayward C, Hernandez D, Hicks AA, Holm H, Hung Y-J, Illig T, Jones MR, Kaleebu P, Kastelein JJP, Khaw K-T, Kim E, Klopp N, Komulainen P, Kumari M, Langenberg C, Lehtimäki T, Lin S-Y, Lindström J, Loos RJF, Mach F, Ardle WLM, Meisinger C, Mitchell BD, Müller G, Nagaraja R, Narisu N, Nieminen TVM, Nsubuga RN, Olafsson I, Ong KK, Palotie A, Papamarkou T, Pomilla C, Pouta A, Rader DJ, Reilly MP, Ridker PM, Rivadeneira F, Rudan I, Ruokonen A, Samani N, Scharnagl H, Seeley J, Silander K, Stančáková A, Stirrups K, Swift AJ, Tiret L, Uitterlinden AG, van Pelt LJ, Vedantam S, Wainwright N, Wijmenga C, Wild SH, Willemsen G, Wilsgaard T, Wilson JF, Young EH, Zhao JH, Adair LS, Arveiler D, Assimes TL, Bandinelli S, Bennett F, Bochud M, Boehm BO, Boomsma DI, Borecki IB, Bornstein SR, Bovet P, Burnier M, Campbell H, Chakravarti A, Chambers JC, Chen Y-DI, Collins FS, Cooper RS, Danesh J, Dedoussis G, de Faire U, Feranil AB, Ferrières J, Ferrucci L, Freimer NB, Gieger C, Groop LC, Gudnason V, Gyllensten U, Hamsten A, Harris TB, Hingorani A, Hirschhorn JN, Hofman A, Hovingh GK, Hsiung CA, Humphries SE, Hunt SC, Hveem K, Iribarren C, Järvelin M-R, Jula A, Kähönen M, Kaprio J, Kesäniemi A, Kivimaki M, Kooner JS, Koudstaal PJ, Krauss RM, Kuh D, Kuusisto J, Kyvik KO, Laakso M, Lakka TA, Lind L, Lindgren CM, Martin NG, März W, Mc Carthy MI, Mc Kenzie CA, Meneton P, Metspalu A, Moilanen L, Morris AD, Munroe PB, Njølstad I, Pedersen NL, Power C, Pramstaller PP, Price JF, Psaty BM, Quertermous T, Rauramaa R, Saleheen D, Salomaa V, Sanghera DK, Saramies J, Schwarz PEH, Sheu WH-H, Shuldiner AR, Siegbahn A, Spector TD, Stefansson K, Strachan DP, Tayo BO, Tremoli E, Tuomilehto J, Uusitupa M, van Duijn CM, Vollenweider P, Wallentin L, Wareham NJ, Whitfield JB, Wolffenbuttel BHR, Altshuler D, Ordovas JM, Boerwinkle E, Palmer CNA, Thorsteinsdottir U, Chasman DI, Rotter JI, Franks PW, Ripatti S, Cupples LA, Sandhu MS, Rich SS, Boehnke M, Deloukas P, Mohlke KL, Ingelsson E, Abecasis GR, Daly MJ, Neale BM, Kathiresan S, Common variants associated with plasma triglycerides and risk for coronary artery disease. Nat. Genet. 45, 1345–1352 (2013). [PubMed: 24097064]
3. Korn ED, Clearing factor, a heparin-activated lipoprotein lipase. I. Isolation and characterization of the enzyme from normal rat heart. J. Biol. Chem. 215, 1–14 (1955). [PubMed: 14392137]
4. Davies BS, Beigneux AP, Barnes II RH, Tu Y, Gin P, Weinstein MM, Nobumori C, Nyren R, Goldberg I, Olivecrona G, Bensadoun A, Young SG, Fong LG, GPIHBP1 is responsible for the entry of lipoprotein lipase into capillaries. Cell Metab. 12, 42–52 (2010). [PubMed: 20620994]
5. Beigneux AP, Davies BS, Gin P, Weinstein MM, Farber E, Qiao X, Peale F, Bunting S, Walzem RL, Wong JS, Blaner WS, Ding ZM, Melford K, Wongsiriroj N, Shu X, de Sauvage F, Ryan RO, Fong LG, Bensadoun A, Young SG, Glycosylphosphatidylinositol-anchored high-density lipoprotein-binding protein 1 plays a critical role in the lipolytic processing of chylomicrons. Cell Metab. 5, 279–291 (2007). [PubMed: 17403372]
6. Goulbourne CN, Gin P, Tatar A, Nobumori C, Hoenger A, Jiang H, Grovenor CR, Adeyo O, Esko JD, Goldberg IJ, Reue K, Tontonoz P, Bensadoun A, Beigneux AP, Young SG, Fong LG, The GPIHBP1-LPL complex is responsible for the margination of triglyceride-rich lipoproteins in capillaries. Cell Metab. 19, 849–860 (2014). [PubMed: 24726386]

7. Doolittle MH, Ben-Zeev O, Elovson J, Martin D, Kirchgessner TG, The response of lipoprotein lipase to feeding and fasting. Evidence for posttranslational regulation. J. Biol. Chem. 265, 4570–4577 (1990). [PubMed: 2307676]
8. Zhang R, Zhang K, An updated ANGPTL3–4-8 model as a mechanism of triglyceride partitioning between fat and oxidative tissues. Prog. Lipid Res. 85, 101140 (2022). [PubMed: 34793860]
9. Dijk W, Kersten S, Regulation of lipid metabolism by angiopoietin-like proteins. Curr. Opin. Lipidol. 27, 249–256 (2016). [PubMed: 27023631]
10. Chen YQ, Pottanat TG, Siegel RW, Ehsani M, Qian YW, Zhen EY, Regmi A, Roell WC, Guo H, Luo MJ, Gimeno RE, Van't Hooft F, Konrad RJ, Angiopoietin-like protein 8 differentially regulates ANGPTL3 and ANGPTL4 during postprandial partitioning of fatty acids. J. Lipid Res. 61, 1203–1220 (2020). [PubMed: 32487544]
11. Sylvers-Davie KL, Davies BSJ, Regulation of lipoprotein metabolism by ANGPTL3, ANGPTL4, and ANGPTL8. Am. J. Physiol. Endocrinol. Metab. 321, E493–E508 (2021). [PubMed: 34338039]
12. Chi X, Britt EC, Shows HW, Hjelmaas AJ, Shetty SK, Cushing EM, Li W, Dou A, Zhang R, Davies BSJ, ANGPTL8 promotes the ability of ANGPTL3 to bind and inhibit lipoprotein lipase. Mol. Metab. 6, 1137–1149 (2017). [PubMed: 29031715]
13. Haller JF, Mintah IJ, Shihanian LM, Stevis P, Buckler D, Alexa-Braun CA, Kleiner S, Banfi S, Cohen JC, Hobbs HH, Yancopoulos GD, Murphy AJ, Gusarova V, Gromada J, ANGPTL8 requires ANGPTL3 to inhibit lipoprotein lipase and plasma triglyceride clearance. J. Lipid Res. 58, 1166–1173 (2017). [PubMed: 28413163]
14. Zhang C, Wang G, Zheng Z, Maddipati KR, Zhang X, Dyson G, Williams P, Duncan SA, Kaufman RJ, Zhang K, Endoplasmic reticulum-tethered transcription factor cAMP responsive element-binding protein, hepatocyte specific, regulates hepatic lipogenesis, fatty acid oxidation, and lipolysis upon metabolic stress in mice. Hepatology 55, 1070–1082 (2012). [PubMed: 22095841]
15. Zhang R, The ANGPTL3–4-8 model, a molecular mechanism for triglyceride trafficking. Open Biol. 6, 150272 (2016). [PubMed: 27053679]
16. Kersten S, Angiopoietin-like 3 in lipoprotein metabolism. Nat. Rev. Endocrinol. 13, 731–739 (2017). [PubMed: 28984319]
17. Kersten S, Mandard S, Tan NS, Escher P, Metzger D, Chambon P, Gonzalez FJ, Desvergne B, Wahli W, Characterization of the fasting-induced adipose factor FIAF, a novel peroxisome proliferator-activated receptor target gene. J. Biol. Chem. 275, 28488–28493 (2000). [PubMed: 10862772]
18. Mandard S, Zandbergen F, van Straten E, Wahli W, Kuipers F, Muller M, Kersten S, The fasting-induced adipose factor/angiopoietin-like protein 4 is physically associated with lipoproteins and governs plasma lipid levels and adiposity. J. Biol. Chem. 281, 934–944 (2006). [PubMed: 16272564]
19. Zheng Z, Kim H, Qiu Y, Chen X, Mendez R, Dandekar A, Zhang X, Zhang C, Liu AC, Yin L, Lin JD, Walker PD, Kapatos G, Zhang K, CREBH couples circadian clock with hepatic lipid metabolism. Diabetes 65, 3369–3383 (2016). [PubMed: 27507854]
20. Cefalù AB, Spina R, Noto D, Valenti V, Ingrassia V, Giammanco A, Panno MD, Ganci A, Barbagallo CM, Averna MR, Novel CREB3L3 nonsense mutation in a family with dominant hypertriglyceridemia. Arterioscler. Thromb. Vasc. Biol. 35, 2694–2699 (2015). [PubMed: 26427795]
21. Lee JH, Giannikopoulos P, Duncan SA, Wang J, Johansen CT, Brown JD, Plutzky J, Hegele RA, Glimcher LH, Lee A-H, The transcription factor cyclic AMP-responsive element-binding protein H regulates triglyceride metabolism. Nat. Med. 17, 812–815 (2011). [PubMed: 21666694]
22. Shimizu-Albergine M, Basu D, Kanter JE, Kramer F, Kothari V, Barnhart S, Thornock C, Mullick AE, Clouet-Foraison N, Vaisar T, Heinecke JW, Hegele RA, Goldberg IJ, Bornfeldt KE, CREBH normalizes dyslipidemia and halts atherosclerosis in diabetes by decreasing circulating remnant lipoproteins. J. Clin. Invest. 131, e153285 (2021). [PubMed: 34491909]

23. Pan X, Hussain MM, Bmal1 regulates production of larger lipoproteins by modulating cAMP-responsive element-binding protein H and apolipoprotein AIV. Hepatology 76, 78–93 (2022). [PubMed: 34626126]
24. Zhang K, Shen X, Wu J, Sakaki K, Saunders T, Rutkowski DT, Back SH, Kaufman RJ, Endoplasmic reticulum stress activates cleavage of CREBH to induce a systemic inflammatory response. Cell 124, 587–599 (2006). [PubMed: 16469704]
25. Brown MS, Goldstein JL, A proteolytic pathway that controls the cholesterol content of membranes, cells, and blood. Proc. Natl. Acad. Sci. U.S.A. 96, 11041–11048 (1999). [PubMed: 10500120]
26. Kim H, Mendez R, Zheng Z, Chang L, Cai J, Zhang R, Zhang K, Liver-enriched transcription factor CREBH interacts with peroxisome proliferator-activated receptor α to regulate metabolic hormone FGF21. Endocrinology 155, 769–782 (2014). [PubMed: 24424044]
27. Kim H, Zheng Z, Walker PD, Kapatos G, Zhang K, CREBH maintains circadian glucose homeostasis by regulating hepatic glycogenolysis and gluconeogenesis. Mol. Cell. Biol. 37, e00048–e00017 (2017). [PubMed: 28461393]
28. Lee M-W, Chanda D, Yang J, Oh H, Kim SS, Yoon Y-S, Hong S, Park K-G, Lee I-K, Choi C-S, Hanson RW, Choi HS, Koo S-H, Regulation of hepatic gluconeogenesis by an ER-bound transcription factor, CREBH. Cell Metab. 11, 331–339 (2010). [PubMed: 20374965]
29. Kim H, Williams D, Qiu Y, Song Z, Yang Z, Kimler V, Goldberg A, Zhang R, Yang Z, Chen X, Wang L, Fang D, Lin JD, Zhang K, Regulation of hepatic autophagy by stress-sensing transcription factor CREBH. FASEB J. 33, 7896–7914 (2019). [PubMed: 30912978]
30. Nakagawa Y, Satoh A, Yabe S, Furusawa M, Tokushige N, Tezuka H, Mikami M, Iwata W, Shingyouchi A, Matsuzaka T, Kiwata S, Fujimoto Y, Shimizu H, Danno H, Yamamoto T, Ishii K, Karasawa T, Takeuchi Y, Iwasaki H, Shimada M, Kawakami Y, Urayama O, Sone H, Takekoshi K, Kobayashi K, Yatoh S, Takahashi A, Yahagi N, Suzuki H, Yamada N, Shimano H, Hepatic CREB3L3 controls whole-body energy homeostasis and improves obesity and diabetes. Endocrinology 155, 4706–4719 (2014). [PubMed: 25233440]
31. Jensen-Cody SO, Potthoff MJ, Hepatokines and metabolism: Deciphering communication from the liver. Mol. Metab. 44, 101138 (2021). [PubMed: 33285302]
32. Priest C, Tontonoz P, Inter-organ cross-talk in metabolic syndrome. Nat. Metab. 1, 1177–1188 (2019). [PubMed: 32694672]
33. Paigen B, Morrow A, Holmes PA, Mitchell D, Williams RA, Quantitative assessment of atherosclerotic lesions in mice. Atherosclerosis 68, 231–240 (1987). [PubMed: 3426656]
34. Matsuzawa N, Takamura T, Kurita S, Misu H, Ota T, Ando H, Yokoyama M, Honda M, Zen Y, Nakanuma Y, Miyamoto K-I, Kaneko S, Lipid-induced oxidative stress causes steatohepatitis in mice fed an atherogenic diet. Hepatology 46, 1392–1403 (2007). [PubMed: 17929294]
35. Pang ZP, Sudhof TC, Cell biology of Ca^{2+}–triggered exocytosis. Curr. Opin. Cell Biol. 22, 496–505 (2010). [PubMed: 20561775]
36. Stalder D, Gershlick DC, Direct trafficking pathways from the Golgi apparatus to the plasma membrane. Semin. Cell Dev. Biol. 107, 112–125 (2020). [PubMed: 32317144]
37. Südhof TC, Rothman JE, Membrane fusion: Grappling with SNARE and SM proteins. Science 323, 474–477 (2009). [PubMed: 19164740]
38. Gu Y, Huganir RL, Identification of the SNARE complex mediating the exocytosis of NMDA receptors. Proc. Natl. Acad. Sci. U.S.A. 113, 12280–12285 (2016). [PubMed: 27791016]
39. Ozcan L, Wong CC, Li G, Xu T, Pajvani U, Park SK, Wronska A, Chen BX, Marks AR, Fukamizu A, Backs J, Singer HA, Yates JR 3rd, Accili D, Tabas I, Calcium signaling through CaMKII regulates hepatic glucose production in fasting and obesity. Cell Metab. 15, 739–751 (2012). [PubMed: 22503562]
40. Wang Y, Yan S, Xiao B, Zuo S, Zhang Q, Chen G, Yu Y, Chen D, Liu Q, Liu Y, Shen Y, Yu Y, Prostaglandin $F_{2\alpha}$ facilitates hepatic glucose production through CaMKIIγ/p38/FOXO1 signaling pathway in fasting and obesity. Diabetes 67, 1748–1760 (2018). [PubMed: 29773555]
41. Easom RA, CaM kinase II: A protein kinase with extraordinary talents germane to insulin exocytosis. Diabetes 48, 675–684 (1999). [PubMed: 10102681]

42. Easom RA, Filler NR, Ings EM, Tarpley J, Landt M, Correlation of the activation of Ca^{2+}/calmodulin-dependent protein kinase II with the initiation of insulin secretion from perifused pancreatic islets. Endocrinology 138, 2359–2364 (1997). [PubMed: 9165023]
43. Sheng M, Thompson MA, Greenberg ME, CREB: A Ca^{2+}-regulated transcription factor phosphorylated by calmodulin-dependent kinases. Science 252, 1427–1430 (1991). [PubMed: 1646483]
44. Ishiguro K, Green T, Rapley J, Wachtel H, Giallourakis C, Landry A, Cao Z, Lu N, Takafumi A, Goto H, Daly MJ, Xavier RJ, Ca^{2+}/calmodulin-dependent protein kinase II is a modulator of CARMA1-mediated NF-κB activation. Mol. Cell. Biol. 26, 5497–5508 (2006). [PubMed: 16809782]
45. Liu C, Hermann TE, Characterization of ionomycin as a calcium ionophore. J. Biol. Chem. 253, 5892–5894 (1978). [PubMed: 28319]
46. Tsui J, Inagaki M, Schulman H, Calcium/calmodulin-dependent protein kinase II (CaMKII) localization acts in concert with substrate targeting to create spatial restriction for phosphorylation. J. Biol. Chem. 280, 9210–9216 (2005). [PubMed: 15582994]
47. Lee EC, Desai U, Gololobov G, Hong S, Feng X, Yu X-C, Gay J, Wilganowski N, Gao C, Du L-L, Chen J, Hu Y, Zhao S, Kirkpatrick L, Schneider M, Zambrowicz BP, Landes G, Powell DR, Sonnenburg WK, Identification of a new functional domain in angiopoietin-like 3 (ANGPTL3) and angiopoietin-like 4 (ANGPTL4) involved in binding and inhibition of lipoprotein lipase (LPL). J. Biol. Chem. 284, 13735–13745 (2009). [PubMed: 19318355]
48. Wu SA, Kersten S, Qi L, Lipoprotein lipase and its regulators: An unfolding story. Trends Endocrinol. Metab. 32, 48–61 (2021). [PubMed: 33277156]
49. Dron JS, Dilliott AA, Lawson A, McIntyre AD, Davis BD, Wang J, Cao H, Movsesyan I, Malloy MJ, Pullinger CR, Kane JP, Hegele RA, Loss-of-function *CREB3L3* variants in patients with severe hypertriglyceridemia. Arterioscler. Thromb. Vasc. Biol. 40, 1935–1941 (2020). [PubMed: 32580631]
50. Sampieri L, Di Giusto P, Alvarez C, CREB3 transcription factors: ER-Golgi stress transducers as hubs for cellular homeostasis. Front. Cell Dev. Biol. 7, 123 (2019). [PubMed: 31334233]
51. Khan HA, Margulies CE, The role of mammalian Creb3-like transcription factors in response to nutrients. Front. Genet. 10, 591 (2019). [PubMed: 31293620]
52. Ye J, Transcription factors activated through RIP (regulated intramembrane proteolysis) and RAT (regulated alternative translocation). J. Biol. Chem. 295, 10271–10280 (2020). [PubMed: 32487748]
53. McCurdy EP, Chung KM, Benitez-Agosto CR, Hengst U, Promotion of axon growth by the secreted end of a transcription factor. Cell Rep. 29, 363–377.e5 (2019). [PubMed: 31597097]
54. Saito A, Kanemoto S, Zhang Y, Asada R, Hino K, Imaizumi K, Chondrocyte proliferation regulated by secreted luminal domain of ER stress transducer BBF2H7/CREB3L2. Mol. Cell 53, 127–139 (2014). [PubMed: 24332809]
55. Jin N, Matter WF, Michael LF, Qian Y, Gheyi T, Cano L, Perez C, Lafuente C, Broughton HB, Espada A, The angiopoietin-like protein 3 and 8 complex interacts with lipoprotein lipase and induces LPL cleavage. ACS Chem. Biol. 16, 457–462 (2021). [PubMed: 33656326]
56. Fu Z, Abou-Samra AB, Zhang R, A lipasin/Angptl8 monoclonal antibody lowers mouse serum triglycerides involving increased postprandial activity of the cardiac lipoprotein lipase. Sci. Rep. 5, 18502 (2016).
57. Luebke-Wheeler J, Zhang K, Battle M, Si-Tayeb K, Garrison W, Chhinder S, Li J, Kaufman RJ, Duncan SA, Hepatocyte nuclear factor 4α is implicated in endoplasmic reticulum stress-induced acute phase response by regulating expression of cyclic adenosine monophosphate responsive element binding protein H. Hepatology 48, 1242–1250 (2008). [PubMed: 18704925]
58. Cushing EM, Chi X, Sylvers KL, Shetty SK, Potthoff MJ, Davies BSJ, Angiopoietin-like 4 directs uptake of dietary fat away from adipose during fasting. Mol. Metab. 6, 809–818 (2017). [PubMed: 28752045]
59. de Leeuw CA, Mooij JM, Heskes T, Posthuma D, MAGMA: Generalized gene-set analysis of GWAS data. PLoS Comput. Biol. 11, e1004219 (2015). [PubMed: 25885710]

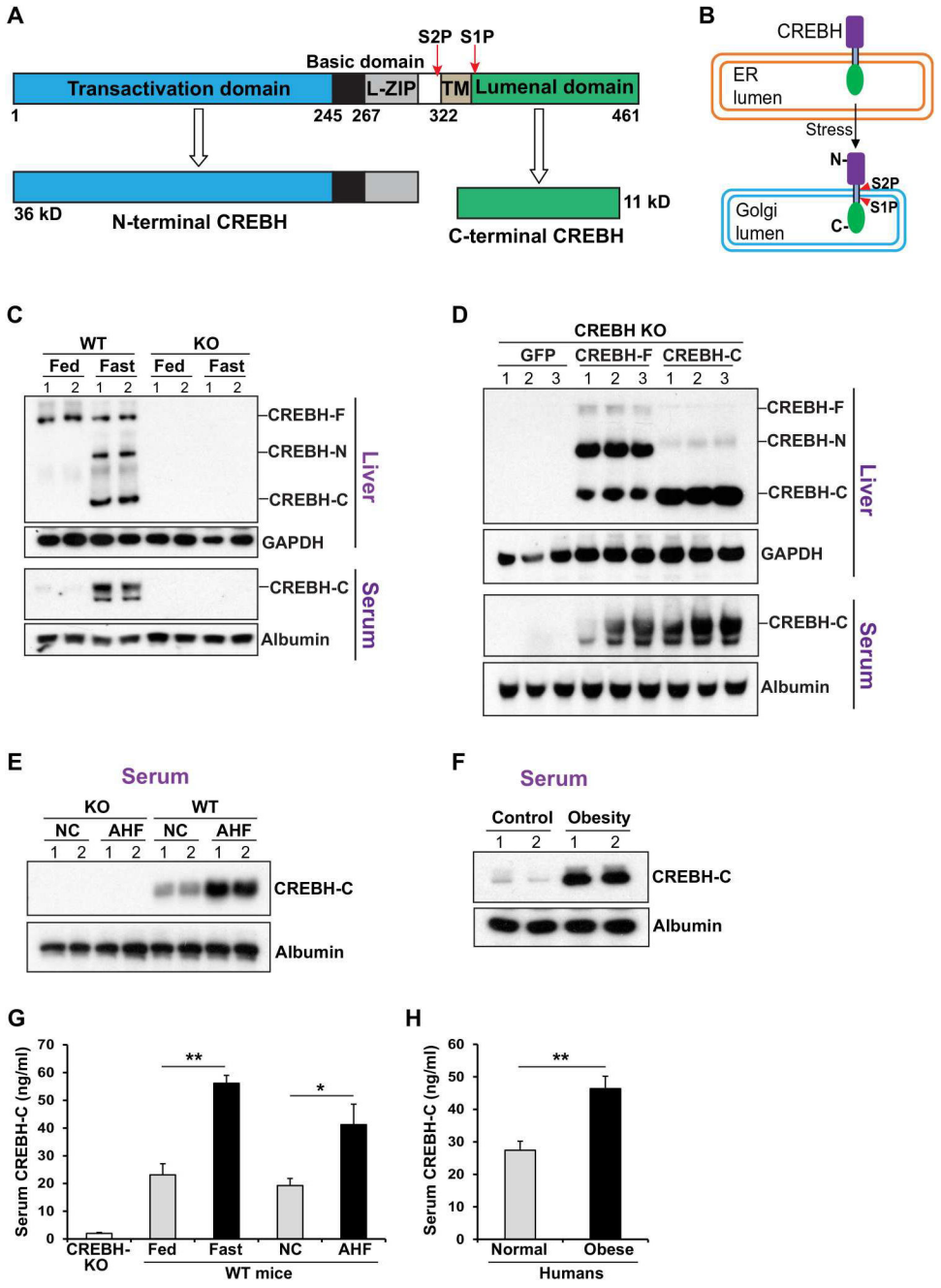

Fig. 1. CREBH is processed to release a C-terminal fragment that is secreted into the blood sera of fasted or atherogenic diet-fed mice or of human patients with obesity.

(**A**) Conserved CREBH protein protease cleavage sites, domain structure, and cleaved N- and C-terminal fragments. (**B**) Membrane-associated topology of CREBH. (**C**) Western blot analysis to detect full-length CREBH (CREBH-F), CREBH N terminus (CREBH-N), and CREBH-C in the livers or blood sera of fed or fasted (14 hours) wild-type (WT) and CREBH-KO mice. Liver lysate and blood serum samples were immunoblotted for GAPDH and albumin as the loading controls. Each lane represents an individual mouse. (**D**) Western blot analysis to detect CREBH-F, CREBH-N, and CREBH-C in the livers or blood sera of

CREBH-KO mice injected with adenoviruses overexpressing GFP, CREBH-F, or CREBH-C. GAPDH and albumin were used as the loading controls for liver lysate and blood serum samples, respectively. Each lane represents an individual mouse. (**E**) Western blot analysis to detect CREBH-C and albumin in the blood sera of CREBH-KO and WT mice fed an AHF or NC for 6 months. Each lane represents an individual mouse. (**F**) Western blot analysis to detect CREBH-C and albumin proteins in the blood sera of human obese and control patients (eight sera per group pooled into two wells). (**G** and **H**) Concentrations of CREBH-C in the blood sera of CREBH-KO mice, of WT mice in the fed or fasted (14-hour) state, of WT mice fed NC or an AHF diet for 6 months (G), and of human patients with obesity or healthy controls (H), as determined by ELISA. Means ± SEM ($n = 4$ mice or individuals per group). *$P \leq 0.05$; **$P \leq 0.01$.

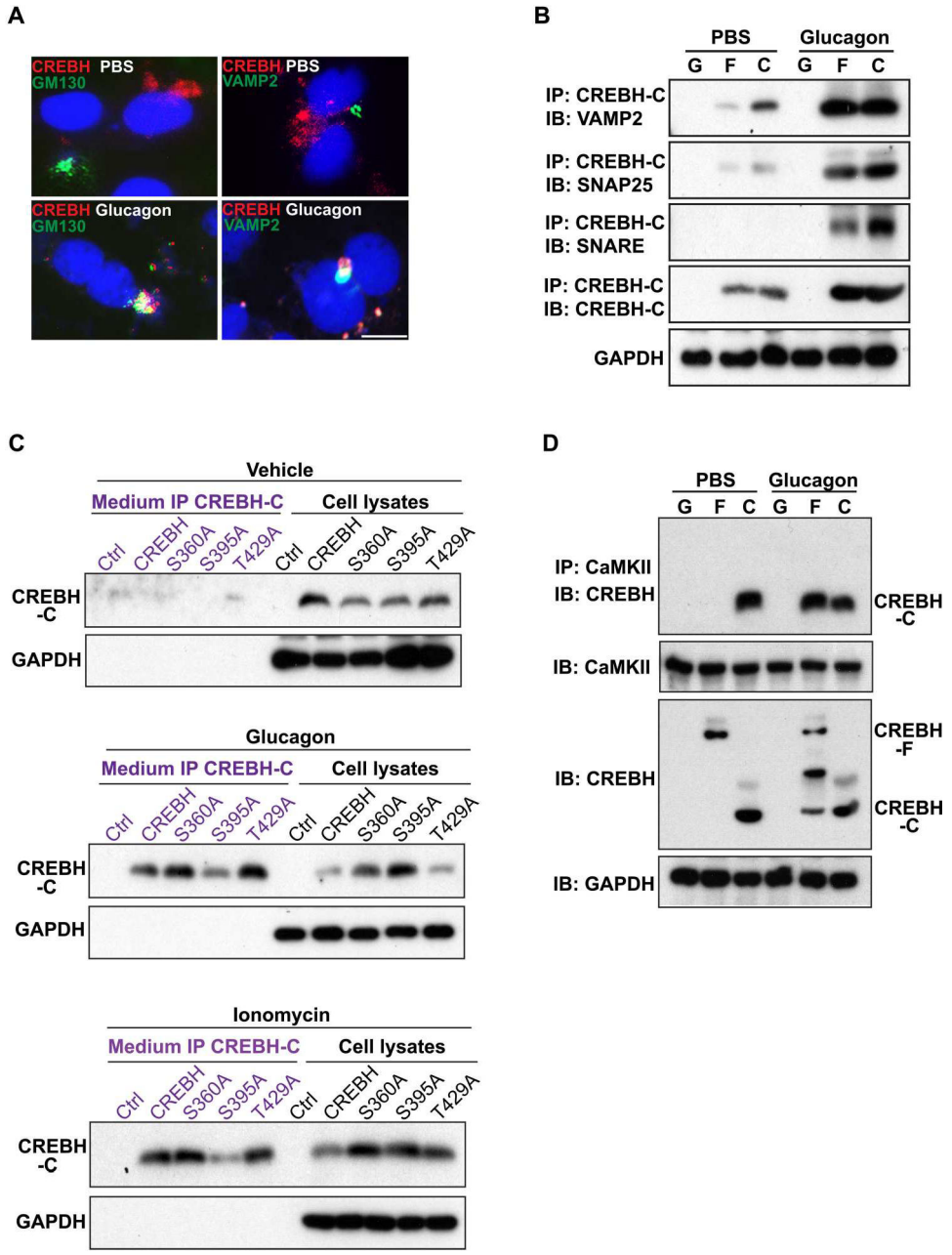

Fig. 2. Secretion of CREBH-C occurs through the exocytotic pathway and is regulated by CaMKII-mediated phosphorylation.

(**A**) Immunofluorescence labeling and confocal microscopy of the Golgi compartment marker GM130 (green), VAMP2-positive exocytotic vesicles (green), and CREBH-C (red) in Huh7 cells transduced with adenovirus encoding Flag-tagged CREBH-F. CREBH-expressing Huh7 cells were treated with glucagon (25 nM) or PBS for 4 hours. Scale bar, 100 μm. Images are representative of three independent experiments. (**B**) CREBH-C immunoprecipitates from Huh7 cells expressing GFP (G), CREBH-F (F), or CREBH-C (C) and treated with glucagon (25 nM) or PBS for 6 hours were immunoblotted for VAMP2, SNAP25, SNARE, or CREBH-C. Lysates were immunoblotted for GAPDH as the loading

control. Immunoblots are representative of three independent experiments. (**C**) Huh7 cells expressing nonmutated human CREBH (CREBH) or the S360A, S395A, or T429A mutants were treated with PBS, glucagon (25 nM), or ionomycin (1 μM) for 6 hours. Lysates were immunoblotted to detect intracellular CREBH-C. CREBH-C immunoprecipitates from the cell culture media were immunoblotted to detect secreted CREBH-C. Immunoblots are representative of three independent experiments. (**D**) CaMKII immunoprecipitates from Huh7 cells expressing GFP, CREBH-F (F), or CREBH-C (C) and treated with glucagon (25 nM) or PBS for 6 hours were immunoblotted for CREBH-C. Lysates were immunoblotted for CaMKII, CREBH, and GAPDH. Immunoblots are representative of three independent experiments. IP, immunoprecipitation; IB, immunoblotting.

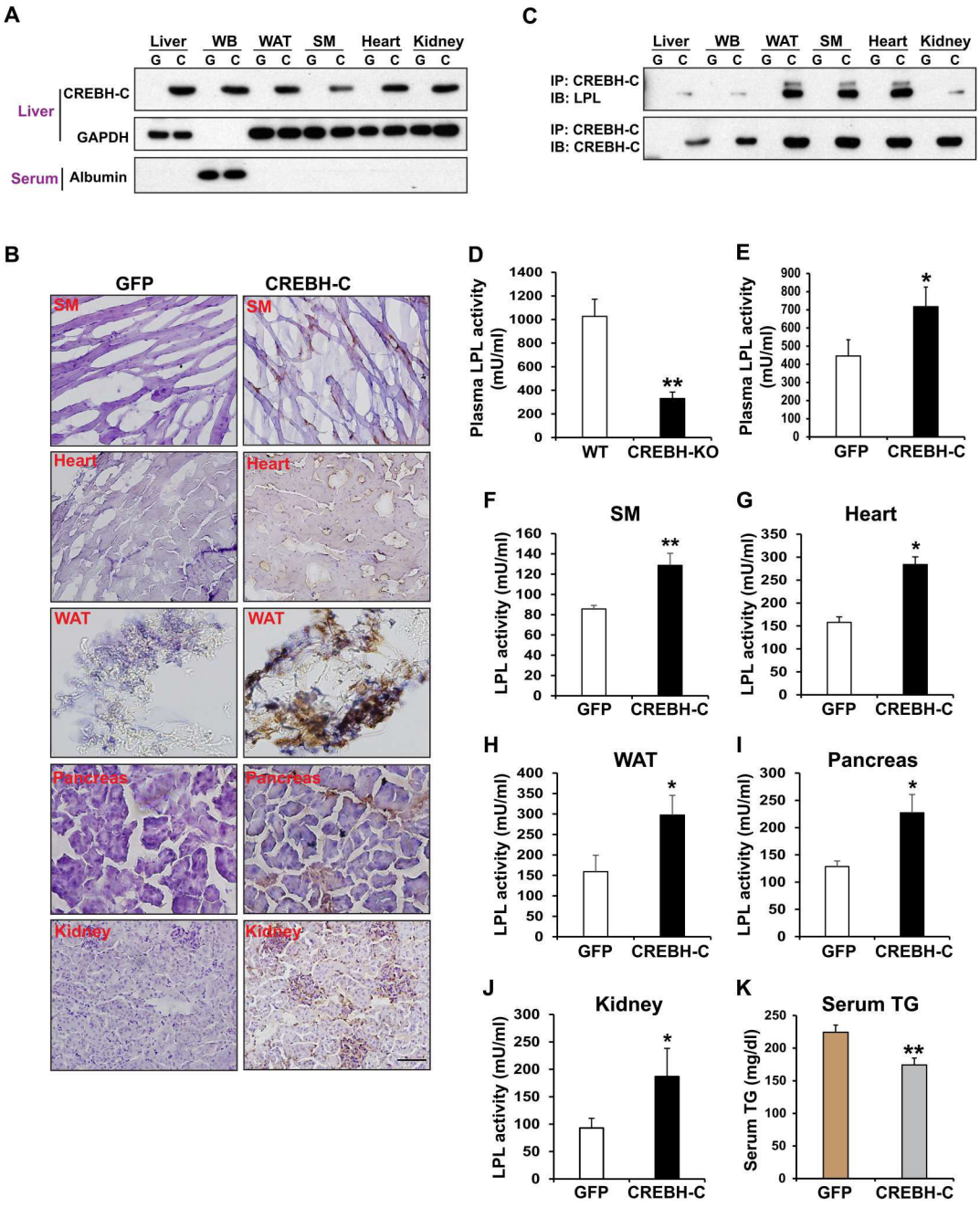

Fig. 3. CREBH-C is transported into the circulation and metabolic organs, where it stimulates tissue-residential or intravascular LPL activities and TG lipolysis.

(**A**) Lysates from the livers, whole blood (WB), WAT, skeletal muscle (SM), hearts, and kidneys of CREBH-KO mice expressing GFP (G) or CREBH-C (C) were immunoblotted for CREBH-C and for GAPDH and albumin as the loading controls for tissue protein lysate and blood serum samples, respectively. Immunoblots are representative of six mice for each group. (**B**) IHC staining of CREBH-C in the SM, heart, WAT, pancreas, and kidney sections of CREBH-KO mice expressing GFP or CREBH-C. Scale bar, 50 μm. Images are representative of six mice per group. (**C**) CREBH-C immunoprecipitates from the livers,

WB, WAT, SM, hearts, and kidneys of CREBH-KO mice expressing GFP (G) or CREBH-C (C) were immunoblotted for CREBH-C and LPL. Immunoblots are representative of six mice for each group. (**D**) CREBH-KO and WT control mice were fasted for 14 hours and treated with heparin (1 U/g body weight) for 15 min to release LPL into the blood. LPL lipase activity was measured in blood samples. Data are presented as means ± SEM (n = 8 mice per group; $^{**}P \leq 0.01$). (**E**) Plasma LPL activity after heparin treatment in CREBH-KO mice expressing CREBH-C or GFP. Means ± SEM (n = 6 mice per group; $^{*}P \leq 0.05$). (**F** to **J**) LPL activity in the SM, heart, WAT, pancreas, and kidneys of CREBH-KO mice expressing CREBH-C or GFP. Data are presented as means ± SEM (n = 3 mice per group; $^{*}P \leq 0.05$; $^{**}P \leq 0.01$). (**K**) Serum TG levels of CREBH-KO mice expressing CREBH-C or GFP. Means ± SEM (n = 6 mice per group; $^{**}P \leq 0.01$).

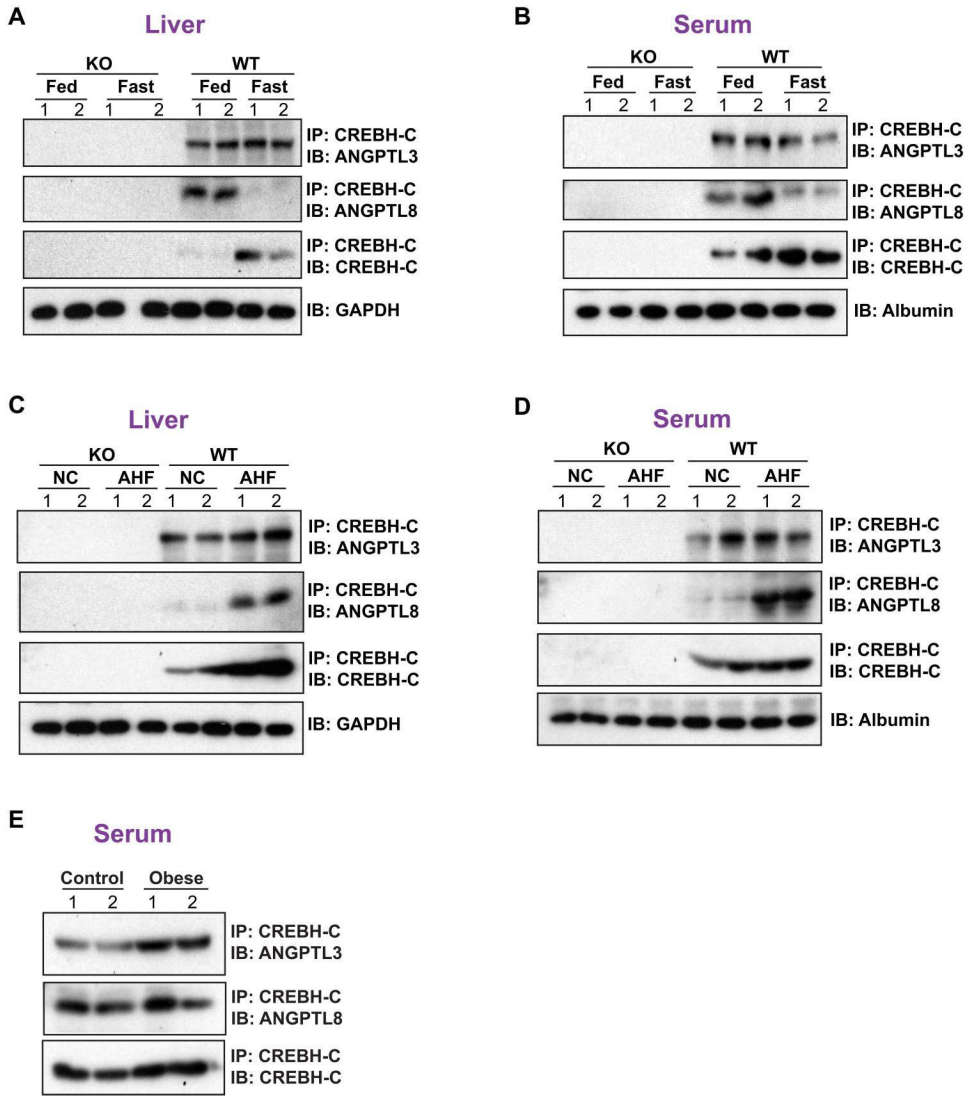

Fig. 4. CREBH-C interacts with ANGPTL3 and ANGPTL8 in the livers or blood sera of fasted or AHF-fed mice and of human patients with obesity.

(**A** and **B**) CREBH-C immunoprecipitates from the livers (A) or blood sera (B) of fed or fasted (14 hours) CREBH-KO and WT mice were immunoblotted for ANGPTL3 or ANGPTL8. Liver protein lysates and blood serum samples were immunoblotted for GAPDH or albumin, respectively, as the loading controls. Each lane represents an individual mouse. (**C** and **D**) CREBH-C immunoprecipitates from the livers (C) or blood sera (D) of CREBH-KO and WT mice fed NC or an AHF diet for 6 months were immunoblotted for ANGPTL3 or ANGPTL8. Liver protein lysates and blood serum samples were immunoblotted for GAPDH or albumin, respectively, as the loading controls. Each lane represents an individual mouse. (**E**) CREBH-C immunoprecipitates from the blood sera of human obese and control patients (eight sera per group pooled into two wells) were immunoblotted for ANGPTL3, ANGPTL8, or CREBH-C. Blood serum samples were immunoblotted for albumin as the loading control.

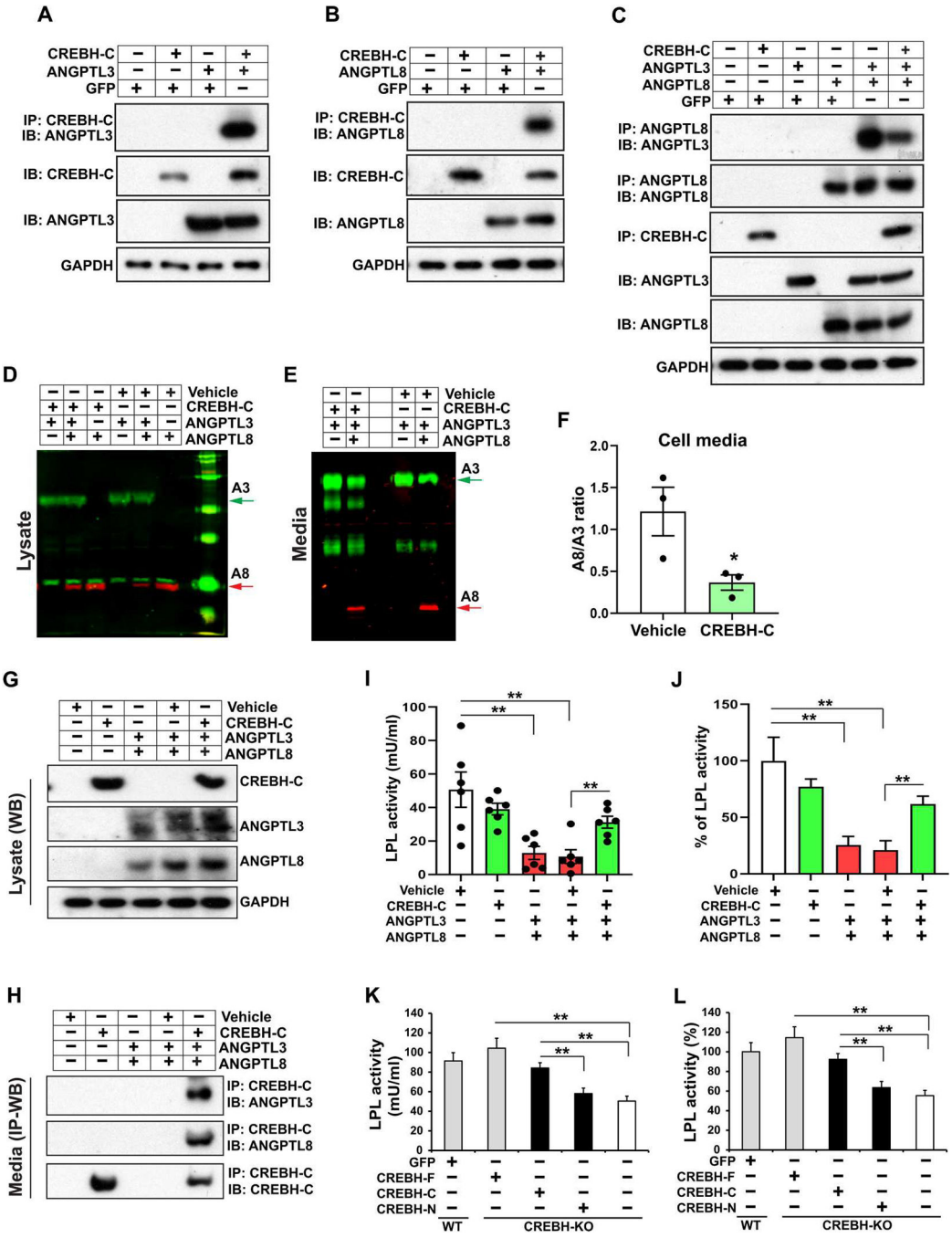

Fig. 5. CREBH-C suppresses the formation of the ANGPTL3/8 complex and enhances LPL activity by attenuating the inhibitory effect of ANGPTL3/8 on LPL.

(**A** to **C**) CREBH-C immunoprecipitates from Huh7 cells overexpressing GFP, CREBH-C, ANGPTL3, and/or ANGPTL8 were immunoblotted for ANGPTL3 (A), ANGPTL8 (B), and ANGPTL3 and ANGPTL8 (C). Lysates or immunoprecipitates were immunoblotted for CREBH-C, ANGPTL3, ANGPTL8, and GAPDH. Immunoblots are representative of three independent experiments. (**D** and **E**) Control or CREBH-C–expressing 293T cells were cotransfected with plasmids expressing ANGPTL3 (tagged with StrepII tag)

and ANGPTL8 (tagged with V5) or both ANGPTL3 and ANGPTL8. Cell lysates or culture media were immunoblotted to detect cellular (D) or secreted (E) ANGPTL3 and ANGPTL8 using antibodies against StrepII and V5 and imaged with a Li-COR Odyssey CLx scanner. Immunoblots are representative of three independent experiments. (**F**) The ratios of ANGPTL8 to ANGPTL3 proteins in the media of the CREBH-C–expressing and vehicle control–expressing 293T cells expressing ANGPTL3 and ANGPTL8, based on the protein signals obtained in the experiments described in (E). Data are presented as means ± SEM ($n = 3$ independent experiments; $*P \leq 0.05$). (**G**) Lysates of 293T cells expressing vector control (vector) or CREBH-C with or without both ANGPTL3 and ANGPTL8 were immunoblotted for CREBH-C, ANGPTL3, and ANGPTL8 at 48 hours after transfection. Immunoblots are representative of three independent experiments. (**H**) CREBH-C immunoprecipitates from the culture media of 293T cells coexpressing vector control or CREBH-C with or without ANGPTL3/8 were immunoblotted for ANGPTL3, ANGPTL8, or CREBH-C. Immunoblots are representative of three independent experiments. (**I**) LPL was incubated with culture media of 293T cells coexpressing vector control or CREBH-C with or without ANGPTL3/8 for 30 min at 37°C as previously described (12). LPL activity was determined using an enzymatic fluorometric LPL assay kit. Data are presented as means ± SEM ($n = 6$ biological replicates per group; $**P \leq 0.01$). (**J**) The degree of LPL inhibition by ANGPTL3 and ANGPTL8 in the presence or absence of CREBH-C was calculated by normalizing LPL activity to that of the positive LPL activity control (the LPL activity of the medium from vector-transfected cells). Data are presented as means ± SEM ($n = 6$ biological replicates per group; $**P \leq 0.01$). (**K**) Activities of LPL after incubation with culture media of WT or CREBH-KO mouse primary hepatocytes reconstituted with CREBH-F, CREBH-C, CREBH-N, or GFP. Culture media of the reconstituted hepatocytes were incubated with LPL, followed by quantitative analysis of LPL lipase activities. Data are presented as means ± SEM ($n = 8$ biological replicates per group; $**P \leq 0.01$). (**L**) Percentages of LPL activities shown in (K). The average LPL activity after incubation with GFP-reconstituted WT hepatocyte media was set as 100%. Means ± SEM ($n = 8$ biological replicates per group; $**P \leq 0.01$).

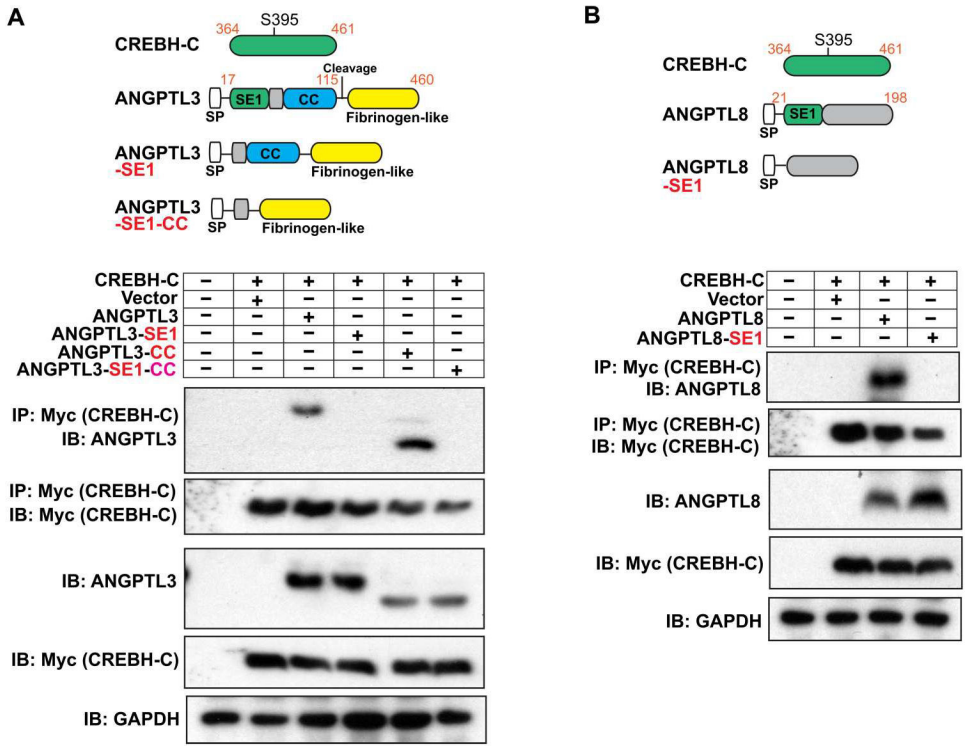

Fig. 6. CREBH-C suppresses the ANGPTL3/8 complex by interacting with ANGPTL3 or ANGPTL8 through the SE1 protein domain.

(**A**) The protein domain structures and truncated forms of ANGPTL3 (top). CC, coiled-coil domain; SP, signal peptide. Myc immunoprecipitates from 293T cells expressing Myc-tagged CREBH-C and ANGPTL3 or its truncated forms were immunoblotted for ANGPTL3 or Myc, and lysates were immunoblotted for GAPDH as the loading control (bottom). ANGPTL3-SE1, ANGPTL3 truncation mutant lacking the SE1 domain; ANGPTL3-SE1-CC, ANGPTL3 truncation mutant lacking both SE1 and CC domains. Immunoblots are representative of three independent experiments. (**B**) The protein domain structures and a truncated form of ANGPTL8 (top). Myc immunoprecipitates from 293T cells expressing Myc-tagged CREBH-C and ANGPTL8 or its truncated forms were immunoblotted for ANGPTL8 or Myc, and lysates were immunoblotted for GAPDH as the loading control (bottom). ANGPTL8-SE1, ANGPTL8 truncation mutant lacking the SE1 domain. Immunoblots are representative of three independent experiments.

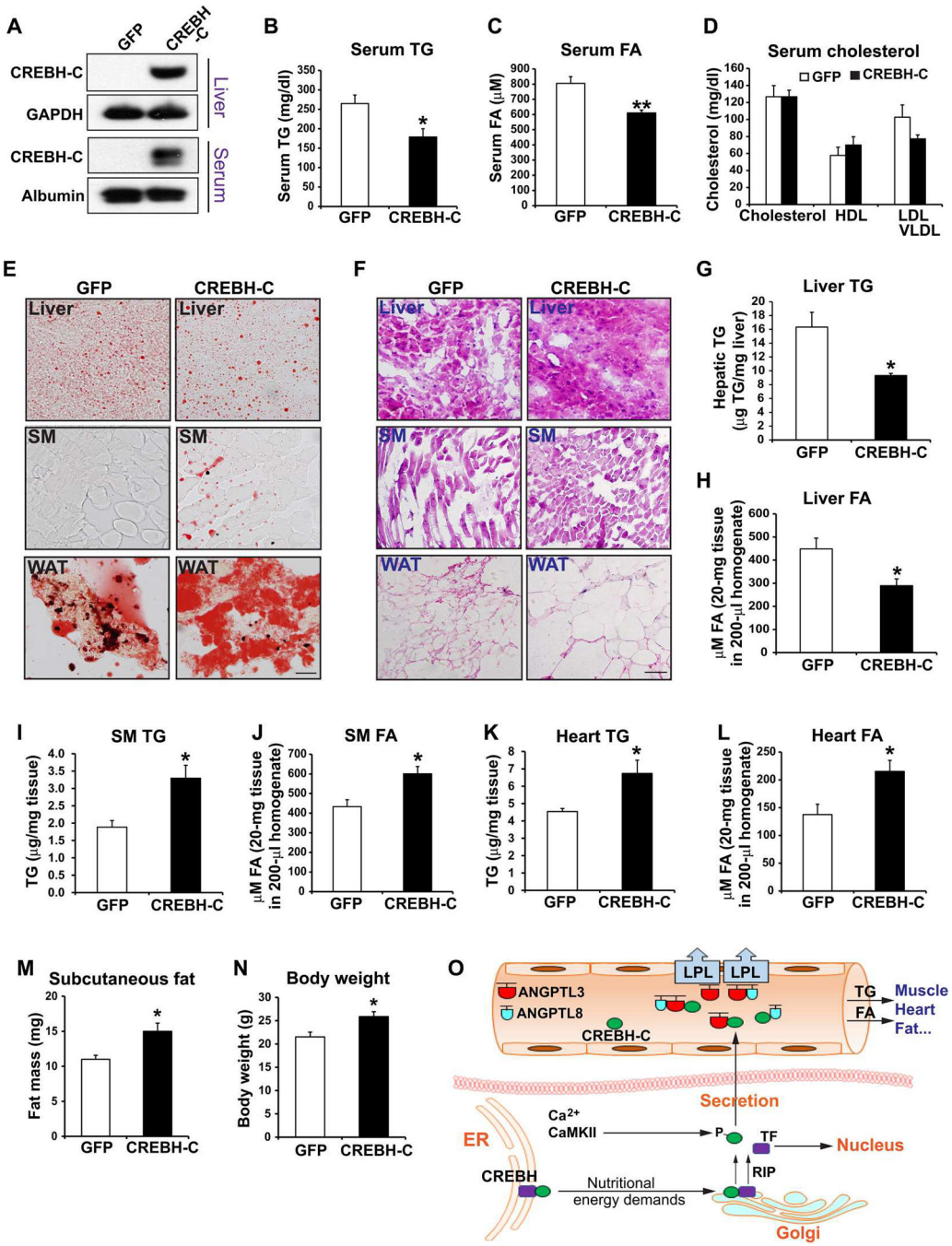

Fig. 7. CREBH-C suppressed hypertriglyceridemia, alleviated hepatic steatosis, and improved lipid partitioning into peripheral tissues in HFD-fed CREBH-KO mice.

CREBH-KO mice fed a HFD for 3 weeks were given adenoviruses to induce CREBH-C or GFP expression in the liver, and HFD feeding continued for an additional 1 week. (**A**) The livers and sera of CREBH-KO mice fed a HFD for 4 weeks were immunoblotted for CREBH-C, GAPDH, and albumin. (**B** to **D**) Serum levels of TG (B), FA (C), total cholesterol (D), HDL (D), and LDL/VLDL (D) were determined in CREBH-KO mice fed a HFD for 4 weeks. Data are presented as means ± SEM (n = 6 mice per group). **P ≤ 0.01.

(**E** and **F**) Oil Red O staining (E) and H&E staining (F) of the livers, SM, and WAT of the HFD-fed CREBH-KO mice expressing GFP or CREBH-C. Scale bars, 50 μm. Images are representative of six mice per group. (**G** to **L**) Quantitative analyses of hepatic TG and FA (G and H), TG and FA contents in the skeletal muscle (I and J), and TG and FA contents in the hearts (K and L) of HFD-fed CREBH-KO mice expressing GFP or CREBH-C. Data are presented as means ± SEM (n = 6 mice per group). (**M** and **N**) Measurements of subcutaneous fat mass (M) and body weights (N) of HFD-fed CREBH-KO mice expressing GFP or CREBH-C. Data are presented as means ± SEM (n = 6 mice per group). *P ≤ 0.05. (**O**) Illustration of the regulatory pathways through which CREBH-C regulates LPL activity and subsequent TG lipolysis and partitioning through inhibitory interactions with ANGPTL3 and ANGPTL8. TF, transcription factor; RIP, regulated intramembrane proteolysis.